An 1 O 2 Route to γ-Hydroxyalkenal Phospholipids by Vitamin E-Induced Fragmentation of Hydroperoxydiene-Derived Endoperoxides

ARTICLE *in* CHEMICAL RESEARCH IN TOXICOLOGY · MAY 2011

Impact Factor: 3.53 · DOI: 10.1021/tx200093m · Source: PubMed

7 AUTHORS, INCLUDING:

Xiaodong Gu
Cleveland Clinic
14 PUBLICATIONS **383** CITATIONS
SEE PROFILE

Wujuan Zhang
Cincinnati Children's Hospital Medical Center
42 PUBLICATIONS **336** CITATIONS
SEE PROFILE

Jaewoo Choi
Oregon State University
22 PUBLICATIONS **121** CITATIONS
SEE PROFILE

James M Laird
private industry (no longer in academia)
19 PUBLICATIONS **166** CITATIONS
SEE PROFILE

Published in final edited form as:
Chem Res Toxicol. 2011 July 18; 24(7): 1080–1093. doi:10.1021/tx200093m.

An $^1O_2$ Route to γ-Hydroxyalkenal Phospholipids by Vitamin E Induced Fragmentation of Hydroperoxydiene-derived Endoperoxides

Xiaodong Gu, **Wujuan Zhang**, **Jaewoo Choi**, **Wei Li**, **Xi Chen**, **James M. Laird**, and **Robert G. Salomon***
Department of Chemistry, Case Western Reserve University, Cleveland, Ohio, 44106

Abstract

Biologically active phospholipids that incorporate an oxidatively truncated acyl chain terminated by a γ-hydroxyalkenal are generated in vivo. The γ-hydroxyalkenal moiety protrudes from lipid bilayers like whiskers that serve as ligands for the scavenger receptor CD36, fostering endocytosis, e.g., of oxidatively damaged photoreceptor cell outer segments by retinal pigmented endothelial cells. They also covalently modify proteins generating carboxyalkyl pyrroles incorporating the ε-amino group of protein lysyl residues. We postulated that γ-hydroxyalkenals could be generated, e.g., in the eye, through fragmentation of hydroperoxy endoperoxides produced in the retina through reactions of singlet molecular oxygen with polyunsaturated phospholipids. Since phospholipid esters are far more abundant in the retina than free fatty acids, we examined the influence of a membrane environment on the fate of hydroperoxy endoperoxides. We now report that linoleate hydroperoxy endoperoxides in thin films and their phospholipid esters in bio-mimetic membranes fragment to γ-hydroxyalkenals, and fragmentation is stoichiometrically induced by vitamin E. The product distribution from fragmentation of the free acid in the homogeneous environment of a thin film is remarkably different than that from the corresponding phospholipid in a membrane. In the membrane, further oxidation of the initially

rgs@case.edu.

[1]The abbreviations used are: $^1O_2$, singlet oxygen; **9,12-diHPODE**, 9,12-dihydroperoxyoctadeca-10,13-dienoic acid; **9-HP-Endo**, 9-hydroperoxy-10,13-epidioxy-11-octadecenoic acid; **9-HPODE**, 9-hydroperoxy-10,12- octadecadienoic acid; **10,13-diHPODE**, 10,13-dihydroperoxyoctadeca-8,11-dienoic acid; **10-HPODE**, 10- hydroperoxy-8,12-octadecadienoic acid; **12-HPODE**, 12-hydroperoxy-9,13-octadecadienoic acid; **13-H-Endo**, 13-hydroxy-9,12-epidioxy-10-octadecenoic acid; **13-HP-Endo**, 13-hydroperoxy-9,12-epidioxy-10-octadecenoic acid; **13-HP-Endo-MiP**, 8-(6-(1-(2-methoxypropan-2-ylperoxy)hexyl)-3,6-dihydro-1,2-dioxin-3-yl)octanoic acid; **13-HP-Endo-PC**, 1-hexadecanoyl-2-(8-(6-(1-hydroperoxyhexyl)-3,6-dihydro-1,2-dioxin-3-yl)octanoyl)-sn-glycero-3-phosphocholine; **13-HP-Endo-PC-MiP**, 1-hexadecanoyl-2-(8-(6-(1-(2-methoxypropan-2- ylperoxy)hexyl)-3,6-dihydro-1,2-dioxin-3-yl)octanoyl)-sn-glycero-3-phosphocholine; **13-HP-MiP**, (9Z,11E)- 13-(2-methoxypropan-2-ylperoxy)octadeca-9,11-dienoic acid; **13-HPODE**, 13-hydroperoxy-9,12-epidioxy-10- octadecenoic acid; **13-HP-PC-MiP**, 1-hexadecanoyl-2-((9Z, 11E)-13-(2-methoxypropan-2-ylperoxy)octadeca-9,11- dienoyl)-sn-glycero-3-phosphocholine; **AMD**, age-related macular degeneration; **CD36**, cluster of differentiation 36; **CEP**, carboxyethylpyrrole; **CML**, N-(carboxymethyl)lysine; **DCC**, dicyclohexylcarbodiimide; **DMAP**, 4- dimethylaminopyridine; **DTPA**, diethylenetriaminepentaacetic acid; **DT-PC**, 1,2-ditridecanoyl-*sn*-glycero-3- phosphatidylcholine; **ESI-MS/MS**, electrospray ionization-tandem mass spectrometry; **FOA**, 8-(furan-2- yl)octanoic acid; **HNE**, 4-hydroxy-2-nonenal; **HODA**, 9-hydroxy-12-oxo-10(E)-dodecenoic acid; **HODA-PC**, 1-hexadecanoyl -2-(9-hydroxy-12-oxo-10(E)-dodecenoyl)-3-phosphatidylcholine; **HODFO**, 8-(2-hydroxy-5- oxo-2,5-dihydrofuran-2-yl)octanoic acid; **HRMS**, high resolution mass spectrometry; **KODA**, 9-keto-12-oxo- 10-dodecenoic acid; **LA**, linoleic acid; **Lyso-PC**, 1-acyl-sn-glycero-3-phosphocholine; **SRM**, selected reaction monitoring; **ODFO**, 8-(5-oxo-2,5-dihydrofuran-2-yl)octanoic acid; **ODFO-PC**, 1-hexadecanoyl-2-(8-(5-oxo- 2,5-dihydrofuran-2-yl)octanoyl)-sn-glycero-3-phosphocholine; **oxPCs**, oxidatively truncated phosphotidylcholines; **oxPEs**, oxidatively truncated phosphotidylethanolamine; **PC**, phosphotidylcholine; **PFB**, pentaflurobenzyl; **PPTs**, pyridinium p-toluene sulfonate; **PUFA**, polyunsaturated fatty acyl; **RPE**, retinal pigment epithelium; **SIR**, selected ion recording; **SP-PC**, 1-stearoyl-2-palmitoyl-sn-glycerol-3-phosphocholine; **SUVs**, small unilamellar vesicles; **TPP**, tetraphenylporphine; **Vit E**, vitamin E.

[2]For a figure summarizing the structures of phospholipids and fatty acids mentioned in this paper, see “Supplementary Information”.

Supporting Information Available: General experimental methods, spectroscopic and analytical data for new compounds.

formed γ-hydroxyalkenal to a butenolide is disfavored. A conformational preference for the γ-hydroxyalkenal, to protrude from the membrane into the aqueous phase, may protect it from oxidation induced by lipid hydroperoxides that remain buried in the lipophilic membrane core.

Introduction

Phospholipids that incorporate an oxidatively truncated acyl chain terminated by a γ-hydroxyalkenal functional array are generated in vivo by oxidative fragmentation of polyunsaturated phospholipids. The γ-hydroxyalkenal moiety protrudes from lipid bilayers like whiskers (1) that serve as ligands for the scavenger receptor CD36[1,2], fostering endocytosis of oxidatively damaged photoreceptor cell outer segments by retinal pigmented endothelial cells (2). The γ-hydroxyalkenal moiety also covalently modifies proteins generating carboxyalkyl pyrroles (Fig. 1) that incorporate the ε-amino group of protein lysyl residues (3, 4). Carboxyethyl pyrroles (CEPs) are especially abundant in retinas from individuals with age-related macular degeneration (AMD) (5). They trigger toll-like receptor-mediated angiogenesis into and destruction of the retina, known as “wet AMD”, causing rapid loss of vision (6–8). They also trigger an immune-mediated destruction of the retina known as “dry AMD”. Thus, mice immunized with CEP-modified mouse albumin develop a dry AMD-like phenotype that includes sub-retinal pigment epithelium (RPE) deposits and RPE lesions mimicking geographic atrophy (9). Apparently γ-hydroxyalkenal-derived oxidative protein modifications, e.g., CEPs, participate in the pathogenesis of AMD (10).

Retina is especially vulnerable to oxidative damage owing to its high proportion of polyunsaturated fatty acyls (PUFAs), high concentration of oxygen, and chronic exposure to light. Exposure of rats to intense visible light results in consumption of PUFAs in the retina, and the production of oxidatively truncated phosphotidylcholines (oxPCs) (2) and phosphotidylethanolamines (oxPEs) (11). Lipid oxidation can involve free radical, enzymatic or singlet oxygen pathways. Ample evidence supports the premise that photo generated singlet oxygen contributes to oxidative injury in the eye. Light initiates an action potential by inducing isomerization of an 11-*cis* to an all-*trans* retinal-protein Shiff base in rhodopsin. This photosensitive receptor is reset through hydrolysis of the Schiff base releasing all-*trans* retinal that is reduced to all-*trans* retinol and, through isomerization, oxidation, and condensation with opsin, the initial Schiff base is regenerated (12). However, before it is reduced to retinol, especially under conditions of oxidative stress where NADH levels are depleted, all-trans retinal can be excited to its triplet state that can transfer energy to molecular oxygen to give singlet oxygen (13, 14).

A reaction of singlet oxygen with linoleic acid (LA) generates the unconjugated hydroperoxyoctadecadienoate (10- and 12-HPODE) regioisomers and the conjugated hydroperoxydienes 9- and 13-HPODE (Fig. 2). Through further reaction with singlet oxygen, 10- and 12-HPODE are transformed into the dihydroperoxydienes 9,12- and 10,13-diHPODE (15), that can undergo fragmentation to give γ-hydroxyalkenals (15–17). A reaction of singlet oxygen with 9- and 13-HPODE delivers hydroperoxy endoperoxides (9- and 13-HP-Endo) (18). The present study was undertaken to determine if PUFA hydroperoxy endoperoxides undergo fragmentation to γ-hydroxyalkenals. Furthermore, because phospholipid esters are far more abundant than free fatty acids, it seemed pertinent to examine the influence of a membrane environment on the fate of hydroperoxy endoperoxides. We now report that linoleate hydroperoxy endoperoxides in thin films and their phospholipid esters in bio-mimetic membranes fragment to give γ-hydroxyalkenals that can be oxidized further to the corresponding butenolides (*vide infra*). Vitamin E promotes the fragmentation and the product distribution from fragmentation of the free acid in the

homogeneous environment of a thin film is remarkably different than that from the corresponding phospholipid in a model membrane.

Experimental Procedures

General Methods

See Supporting Information

Liqid Chromatograph/Mass Spectrometry

LC/ESI/MS/MS analysis of hydroperoxy endoperoxide fragmentation was performed on a Quattro Ultima (Micromass, Wythenshawe, UK) connected to a Waters 2690 solvent delivery system with an auto-injector. The source temperature was maintained at 100 °C, and the desolvation temperature was kept at 200 °C. The drying gas (N_2) was maintained at ca. 450 L/h, and the core flow gas was kept at ca. 50 L/h. The multiplier was set at an absolute value of 500. Optimized parameters for hydroperoxy endoperoxides, and their fragmentation products were obtained with authentic samples. MS scans at m/z 80–1000 were obtained for standard compounds (Table S1 in supporting information).

Argon was used as collision gas at a pressure of 5 psi for MS/MS analysis. For MS/MS analysis, the collision energy was optimized for each compound. For selected reaction monitoring (SRM) experiments, the optimum collision energy (giving the strongest signal) was determined for each m/z parent-daughter ion pair (Table S2 in supporting information). FOA (8-(furan-2-yl)octanoic acid) did not give daughter fragments during collision and, therefore, was monitored by selected ion recording (SIR, m/z = 209).

Online chromatographic separation was achieved using a 150×2.0 mm i.d. Prodigy ODS-5 μm column (Phenomenex, Torrance, CA), using binary solvent gradients - water/acetonitrile or water/methanol supplemented with 0.2 % formic acid or 2 mM NH_4OAc. For the carboxylic acids, the water/acetonitrile gradient started with 35% acetonitrile for 10 min, then rose to 60% in 0.5 min and linearly rose to 75% in 15 min. The gradient was then reversed to 35% acetonitrile in 0.5 min, and held for 6 min. For HODA methoxime derivatives, the methanol/water gradient, supplemented with 2mM NH_4OAc, started with 5 % methanol and rose to 100% methanol in 15 min, then was held at 100% methanol for another 15 min. The gradient was then reversed to 5% methanol in 0.5 min, and held at 5% methanol for 4.5 min before the next run. For ODFO-PFB ester derivatives, the methanol/ water gradient, supplemented with 2mM NH_4OAc, started with 50 % methanol and rose to 100% methanol in 10 min, then was held at 100% methanol for another 15 min. The gradient was then reversed to 50% methanol in 0.5 min, and held for 4.5 min before the next run. For the phospholipids, the methanol/water gradient, supplemented with 0.2% formic acid, started with 85% methanol and rose to 100% in 15 min, then was held at 100% methanol for another 15 min. The gradient was then reversed to 85% methanol in 0.5 min, and held at 85% methanol for 4.5 min before the next run. The solvents were all delivered at 200 μL/min.

(9Z,11E)-13-(2-Methoxypropan-2-ylperoxy)octadeca-9,11-dienoic acid (13-HP-MiP)

13-HPODE (120 mg, 0.38 mmol) and pyridinium p-toluene sulfonate (PPTs, 10 mg) were dissolved in dry CH_2Cl_2 (10 mL). Then 2-methoxypropene (100 uL, excess) was added drop-wise via syringe. The resulting mixture was stirred for 0.5 h under argon. Then solvents were removed by rotary evaporation and the crude product was then flash chromatographed on silica gel eluting with hexane and ethyl acetate (2/1) to afford the pure 13-HP-MiP (114 mg, 30 mmol, yield = 78%), R_f = 0.38 with hexane and ethyl acetate (1/1). ^{1}H NMR (400 MHz, $CDCl_3$): δ 6.41 (dd, J = 15.6, 10.8, 1H), 5.92 (t, J = 10.8, 1H),

5.53 (dd, J = 15.2, 8, 1H), 5.37 (dt, J = 10.8, 7.6, 1H), 4.33 (m, 1H), 3.23 (s, 3H), 2.27 (t, J = 7.6 Hz, 2H), 2.11 (m, 2H), 1.50–1.65 (2H), 1.10–1.40 (22H), 0.81 (t, J = 6.8, 3H). ^{13}C NMR (400 MHz, $CDCl_3$): δ 180.3, 133.1, 133.0, 128.2, 128.1, 104.8, 84.9, 49.4, 34.3, 33.3, 32.0, 29.7, 29.3, 29.2, 27.9, 25.3, 24.8, 23.2, 23.0, 22.7, 14.3. HRMS (FAB) *m/z* $[M+Na]^+$ calcd for $C_{22}H_{40}O_5Na$, 407.2774, found 407.2783.

8-(6-(1-(2-Methoxypropan-2-ylperoxy)hexyl)-3,6-dihydro-1,2-dioxin-3-yl)octanoic acid (13-HP-Endo-MiP)

A solution of 13-HP-MiP (142 mg, 0.37 mmol) and tetraphenylporphine (TPP, 9 mg) in CH_2Cl_2 (60 mL) was cooled to 0 °C in a pyrex photoreaction apparatus. Oxygen was bubbled through the solution through a gas dispersion tube and the mixture illuminated by an internal tungsten lamp (500 W) inside an internal cold finger condenser for 72 h. Then the solvent was removed by rotary evaporation and the crude product was purified by flash chromatography on silica gel eluting with hexane and ethyl acetate (1/1) to get 13-HP-Endo-MiP (102 mg, 0.25 mmol, yield = 68%), R_f = 0.36. ^{1}H NMR (400 MHz, $CDCl_3$): δ 5.90–6.10 (m, 2H), 4.40–4.90 (2H), 4.00–4.20 (1H), 3.14 (s, 3H), 2.32 (t, *J* = 7.2 Hz, 2H), 1.20–1.70 (26H), 0.80–0.90 (3H). HRMS (FAB) *m/z* $[M+Na]^+$ calcd for $C_{22}H_{40}O_7Na$, 439.2672, found 439.2674.

8-(6-(1-Hydroperoxyhexyl)-3,6-dihydro-1,2-dioxin-3-yl)octanoic acid (13-HP-Endo)

13-HP-Endo-MiP (20 mg, 0.048 mmol) and pyridinium p-toluene sulfonate (PPTs, 2 mg) were dissolved in dry methanol (5 mL). The mixture was stirred under argon for 24 h. The solvent was removed by rotary evaporation, and the crude product purified by flash chromatography on silica gel eluting with hexane and ethyl acetate (1/1) to give 13-HP-Endo (9 mg, 0.032 mmol, yield = 67%), R_f = 0.31. ^{1}H NMR (400 MHz, $CDCl_3$): δ 5.90–6.05 (2H), 4.40–4.80 (2H), 4.05–4.21 (1H), 2.35 (t, *J* = 7.2 Hz, 2H), 1.44–1.64 (6H), 1.43–1.20 (14H), 0.80–0.96 (3H). HRMS (FAB) *m/z* $[M+H]^+$ calcd for $C_{18}H_{33}O_6$, 345.2277, found, 345.2274. ESI-MS/MS analysis yielded the following diagnostic fragments: m/z 343.2 $[M – H]^-$, m/z 213, 209, 207, 185, 125, 109, 99 (see supplemental information).

13-HP-Endo was further purified by HPLC using a 250×4.6 mm luna 5μ C18(2) column (Phenomenex, Torrance, CA), with a binary solvent (water and acetonitrile) gradient at 1 mL/min. The gradient started with 60% acetonitrile and rose to 100% acetonitrile linearly in 30 min. The gradient was then reversed to 60% acetonitrile in 0.5 min, and then held for 4.5 min at 60% acetonitrile.

8-(2-Hydroxy-5-oxo-2,5-dihydrofuran-2-yl)octanoic acid (HODFO)

To a magnetically stirred solution of NaH_2PO_4 (110 mg, 0.81 mmol) and $NaClO_2$ (80% purity, 180 mg, 1.59 mmol) in 5 mL t-BuOH/water (5:1) was added FOA (112 mg, 0.53 mmol) in 5 mL t-BuOH/water (5:1) solution in a drop-wise via syringe. The resulting mixture was stirred at room temperature for 1.5 h. Solvents were removed by rotary evaporation, and the crude product was purified by flash chromatography on silica gel eluting with methanol and chloroform (1:10) to give the pure HODFO (102.8 mg, 0.425 mmol, yield = 80%), R_f = 0.25 with 15% methanol in chloroform. ^{1}H NMR (400 MHz, $CDCl_3$): δ 7.10–7.22 (1H), 6.07 (d, J = 6.4 Hz, 1H), 2.24–2.38 (2H), 1.85– 2.05 (2H), 1.50–1.65 (2H), 1.20–1.40 (8H). HRMS (FAB) m/z $[M+Na]^+$ calcd for $C_{12}H_{18}O_5Na$, 265.1052, found 265.1028.

8-(5-Oxo-2,5-dihydrofuran-2-yl)octanoic acid (ODFO)

HODFO (16 mg, 0.066 mmol) was dissolved in methanol (3 mL) and the mixture was cooled in an ice bath. $NaBH_4$ (15 mg, excess) was added in small portions, and the resulting

mixture was stirred for 1 h at room temperature. Water (100 μL) was then added and the mixture was stirred for another 1 h. Then 1 M HCl was added to acidify the solution to pH = 3 and the resulting mixture was stirred at room temperature for 30 min. The product was extracted into $CHCl_3$ (10 mL × 3), and solvents evaporated. Chromatography on silica gel eluting with 5% CH_3OH in $CHCl_3$ delivered pure ODFO (12 mg, 0.053 mmol, yield = 80 %), R_f = 0.25 with 10% methanol in chloroform. ^1H NMR (400 MHz, $CDCl_3$): δ 7.38 (dd, J = 5.6, 1.6 Hz, 1H), 6.05 (dd, J = 6.0, 2.4 Hz, 1H), 4.97 (m, 1H), 2.28 (t, J = 7.6 Hz, 2H), 1.65 (m, 1H), 1.50–1.63 (3H), 1.30–1.42 (2H), 1.20–1.32 (6H). ^{13}C NMR (400 MHz, CD_3OD): δ 176.5, 174.6, 158.4, 120.4, 84.4, 33.7, 32.9, 29.1, 29.0, 28.9, 24.8, 24.8. HRMS (FAB) *m/z* $[M+H]^+$ calcd for $C_{12}H_{19}O_4$, 227.1283, found 227.1274. ESI-MS/MS analysis yielded the following diagnostic fragments: m/z 225.2 $[MH]^-$; m/z 207, 181, 136, 110, 97 (see Fig. 6B).

1-Hexadecanoyl-2-(8-(6-(1-(2-methoxypropan-2-ylperoxy)hexyl)-3,6-dihydro-1,2-dioxin-3-yl)octanoyl)-sn-glycero-3-phosphocholine (13-HP-Endo-PC-MiP)

A solution of 13-HP-PC-MiP (24 mg, 0.027 mmol) and tetraphenylporphine (TPP, 4 mg) in CH_2Cl_2 (50 mL) was cooled to 0 °C in a pyrex photoreaction apparatus. Oxygen was bubbled through the solution through a gas dispersion tube and the mixture was illuminated by an internal tungsten lamp (500 W) inside an internal annular cold finger for 96 h. Solvent was removed by rotary evaporation and the crude product was purified by HPLC using a 250×10.00 mm luna 5 C18(2) semi-preparative column (Phenomenex, Torrance, CA). The column was eluted with methanol/water (100:5, v/v) containing 5 mM NH_4OAc at 5 mL/min. The fractions were collected and analyzed by ESI-MS on Thermo Finnigan LCQ DecaXP instrument in the positive mode using nitrogen as the sheath and auxiliary gas. The heated capillary temperature was 200 °C, the source voltage was 4.50 kV, and the capillary voltage was 20.00 V. 13-HP-PC-MiP (9 mg, 0.01 mmol) was recovered and the title 13-HPEndo- PC-MiP was obtained (9 mg, 0.01 mmol, yield = 58 %). ^1H NMR (400 MHz, $CDCl_3$): δ 5.90 (m, 2H), 5.15 (s, 1H), 3.60–4.80 (11H), 3.30 (s, 9H), 3.25 (s, 3H), 2.16–2.27 (4H), 1.80–2.00 (4H), 1.00–1.60 (42 H), 0.70–0.90 (12H). ESI-MS analysis yielded the following diagnostic peaks: m/z 894.9 $[M+H]^+$, m/z 916.8 $[M+Na]^+$, m/z 823.0 $[M+H–MiP]^+$, m/z 1788.3 $[2M+H]^+$ (see Fig 3.8 B). HRMS (FAB) m/z $[M+H]^+$ calcd for $C_{46}H_{89}NO_{13}P$, 894.6071, found 894.6059.

1-Hexadecanoyl-2-(8-(6-(1-hydroperoxyhexyl)-3,6-dihydro-1,2-dioxin-3-yl)octanoyl)-sn-glycero-3-phosphocholine (13-HP-Endo-PC)

13-HP-Endo-PC-MiP (7.6 mg, 0.0085 mmol) and pyridinium p-toluene sulfonate (PPTs, 3 mg) were dissolved into 5 mL of chloroform/methanol (1/1), and the solution stirred under argon for 24 h. The solvents were then removed by rotary evaporation. The residue was dissolved into water (10 mL) and extracted with chloroform (3×10 mL) to remove the PPTs. The crude product was further purified by HPLC using a 250×4.60 mm luna 5 C18(2) column (Phenomenex, Torrance, CA). The column was eluted with methanol/water (90/10, v/v) containing 5 mM NH_4OAc at 1 mL/min. 13-HP-Endo-PC was obtained (4 mg, 0.0049 mmol, yield = 58%). HRMS (FAB) *m/z* $[M+H]^+$ calcd for $C_{42}H_{81}NO_{12}P$, 822.5496, found 822.5456. ESI-MS/MS analysis yielded the following diagnostic fragments: m/z 822.8 $[M+H]^+$, m/z 184.1 (see supplemental information).

1-Hexadecanoyl-2-(8-(5-oxo-2,5-dihydrofuran-2-yl)octanoyl)-sn-glycero-3-phosphocholine (ODFOPC)

ODFO (24 mg, 0.11 mmol), 1-hexadecanoyl-2-hydroxy-sn-glycero-3-phosphocholine (lyso-PC, 40 mg, 0.08 mmol), dicyclohexylcarbodiimide (DCC, 100 mg, 0.48 mmol) and 4-dimethylaminopyridine (DMAP, 10 mg, 0.08 mmol) were dissolved in dry chloroform (5 mL) and the solution stirred at room temperature for 72 h. Solvents were removed by rotary

evaporation to get crude product, and the residue was purified on a silica gel column ($CHCl_3/CH_3OH/H_2O$ = 16/9/1) to give pure ODFO-PC (30.2 mg, 0.04 mmol, yield = 50%). ^{1}H NMR (400 MHz, $CDCl_3/CD_3OD$): δ 7.58 (dd, J = 5.6, 1.6 Hz, 1H), 6.08 (dd, J = 6.0, 2.4 Hz, 1H), 5.18 (m, 1H), 5.07 (m, 1H), 4.38 (dd, J = 12, 3.2 Hz, 1H), 4.20 (m, 2H), 4.12 (dd, J = 12, 6.4 Hz, 1H), 3.96 (t, J = 6.4 Hz, 2H), 3.57 (m, 2H), 3.20 (s, 9H), 2.32–2.20 (4H), 1.50–1.62 (4H), 1.20–1.40 (34H), 0.84(t, J = 6.8 Hz, 3H). HRMS (FAB) *m/z* $[M+H]^+$ calcd for $C_{36}H_{67}NO_{10}P$, 704.4502, found 704.4503. ESI-MS/MS analysis yielded the following diagnostic fragments: m/z 704.6 $[M+H]^+$, m/z 184.1 (see supplemental information).

Thermal decomposition of the linoleate derived hydroperoxy endoperoxide 13-HP-Endo

Small 3 dram glass vials, each containing 13-HP-Endo (10 μg, 0.03 μmol) as a dry film, were incubated at 37 °C for various times. After incubation, the vials were sealed under argon and kept at −80 °C until LC-MS/MS analysis. For the decomposition of 13-HP-Endo with vitamin E, vials containing 13-HP-Endo (10 μg, 0.03 μmmol) and one equivalent vitamin E as a dry film were incubated at 37 °C for various times. After incubation, the vials were sealed under argon and kept at −80 °C until LC-MS/MS analysis. Vials containing 13-HP-Endo (10 μg, 0.03 μmmol) and various amounts of vitamin E as a dry film were incubated at 37 °C for 2 h. After incubation, the vials were sealed under argon and kept at −80 °C until LC-MS/MS analysis. For the decomposition of 13-HP-Endo with vitamin E and DTPA, vials containing 13-HP-Endo (10 μg, 0.03 μmmol) and various amounts of vitamin E and 5 equivalents of DTPA as a dry film were incubated at 37 °C for 2 h. After incubation, the vials were sealed under argon and kept at −80 °C until LC-MS/MS analysis. Before analysis, 100 μL of internal standard solution (8-(furan-2-yl)-8-oxooctanoic acid, 1ng/μl) in methanol was added and 10 μL of this mixture solution was injected into the LC/MS/MS system each time. The amounts of HODA, ODFO, KODA and FOA were monitored simultaneously.

9-Hydoxy-12-(methoxyimino)dodec-10-enoic acid (HODA methoxime)

To authentic HODA (50 μg) in a small vial was added pyridine (200 μL) containing 2 wt% of methoxylamine hydrochloride. The mixture was kept under argon at room temperature over night. Pyridine was then removed under a stream of argon. The residue was dissolved in 0.5 mL of water (pH = 3), and extracted with ethyl ether (1 mL and then 0.5 mL). Solvent was removed from the extract and the residue analyzed via ESI-MS/MS, producing the following fragments: m/z 256.3 $[M-H]^-$; m/z 197 (see supplemental information).

13-HP-Endo (50 μg, 0.15 μmmol) and one equivalent of vitamin E were incubated as a dry film at 37 °C for 2 h. Then pyridine (200 μL) containing 2 wt% of methoxylamine hydrochloride was added, and the mixture was kept under argon at room temperature over night. Pyridine was then removed under a stream of argon. The residue was then dissolved in 0.5 mL of water (pH = 3), and the solution was extracted with ethyl ether (1 mL and then 0.5 mL). Solvent was then removed from the extract and the residue was sealed under argon and kept at −80 °C until LC-MS/MS analysis.

Perfluorobenzyl 8-(5-oxo-2,5-dihydrofuran-2-yl)octanoate (ODFO-PFB ester)

To authentic ODFO (50 μg) in a small vial was added dry acetonitrile (100 μL) containing 10 wt% of pentafluorobenzyl bromide and 20 wt% of N,N-diisopropylethylamine. The resulting mixture was kept at room temperature for 2 h, and the solvent was removed with a stream of argon. The residue was dissolved in 1 mL of water, and the product was extracted into ethyl acetate (1 mL). ESI-MS/MS analysis in the positive mode gave $[M+NH_4]^+$ and characteristic daughter fragments at m/z 209, 181, 163, 145, 135 (see supplemental information).

13-HP-Endo (50 μg, 0.15 μmmol) and one equivalent of vitamin E were incubated as a dry film at 37 °C for 2 h. Then dry acetonitrile (100 μL) containing 10 wt% of pentafluorobenzyl bromide and 20 wt% of N,N-diisopropylethylamine was added. The mixture was kept under argon at room temperature for 2 h, and solvents removed under a stream of argon. The residue was dissolved in water (1 mL), and the solution was extracted with ethyl acetate (1 mL). Solvent was removed from the extract and the residue was sealed under argon and kept at −80 °C until LC-MS/MS analysis.

Thermal decomposition of linoleate derived hydroperoxy endoperoxide phosphocholine ester 13-HPEndo-PC in a model membrane

Vesicles comprised of 13-HP-Endo-PC and vitamin E were prepared by extrusion by a method described previously (19). Specifically, 13-HP-Endo-PC (100 μg), with 1-stearoyl-2- palmitoyl-*sn*-glycero-3-phosphocholine (SP-PC, 900 μg) as carrier and one equivalent of vitamin E were initially dissolved into methanol, vortexed for 1 min and the solvent removed under a stream of argon. Lipids were fully hydrated by the addition of phosphate saline buffer (1 mL, 50 mM, pH = 7.4) with or without DTPA (100 μM). Following vortexing to disperse the hydrated lipids, small unilamellar vesicles (SUVs) were generated by extrusion through a polycarbonate filter until a clear solution was produced (about 15 times) using an Avanti Mini-Extruder Set (Avanti Polar Lipids, Alabaster, AL). The buffer solution of vesicles was aliquoted into small vials, (100 μL in each) of a buffer solution containing 13-HP-Endo-PC (10 μg), and the vials incubated at 37 °C for various times. After incubation, DT-PC (100 ng) was added as internal standard, and the mixture was immediately extracted by the Bligh & Dyer method. The extracts were sealed under argon and stored in −80°C until LC-MS/MS analysis (less than 24 hours).

Thermal decomposition of linoleate derived hydroperoxy endoperoxide phosphocholine ester 13-HPEndo-PC in homogeneous solution

13-HP-Endo-PC (10 μg), with SP-PC (90 μg) and one equivalent vitamin E was dissolved in a homogeneous mixture of methanol (100 μL) and PBS buffer (100 μL, 50 mM, pH = 7.4). The vial was incubated at 37 °C for 4 hour. After incubation, DT-PC (100 ng) was added as internal standard, and the mixture was immediately extracted by Bligh &Dyer method. The extract was sealed under argon and stored in – 80 °C until LC-MS/MS analysis (less than 24 hours).

Results

Synthesis of a linoleate-derived hydroperoxy endoperoxide and its predicted fragmentation products

We postulated that fragmentation of the hydroperoxy endoperoxide 13-HP-Endo would deliver the γ-hydroxyalkenal HODA through fragmentation of an intermediate alkoxy radical by β-scission in conjunction with homolysis of the dialkyl peroxide and hydrogen atom abstraction to produce the γ-hydroxy alkenal *cis*- HODA (Fig. 3). The *cis* γ-hydroxy alkenal is expected to be unstable. It can isomerize into the *trans* γ-hydroxy alkenal HODA or be oxidized further to the lactone ODFO in the oxidative environment. The unsaturated aldehyde HODA can also be oxidized further, e.g., to deliver KODA (Fig. 3) (20, 21). We previously found that a HODA ester of 2-lysophosphatidylcholine cyclizes and loses one molecule of water to give a PC ester of the furan FOA under biomimetic reaction conditions presumably through prior isomerization to *cis*-HODA (22).

A structurally nonspecific synthesis of linoleate-derived hydroperoxy endoperoxides was accomplished previously by treating a mixture of linoleate 9- and 13-hydroperoxyoctadecadienoate (9- and 13-HPODE) with singlet oxygen, generated by

gaseous O_2 in the presence of photosensitizer (18). Isolation of the pure hydroperoxy endoperoxides from the complex reaction product mixture required tedious HPLC. However, the reaction with singlet molecular oxygen is quite slow, and requires many days of irradiation to achieve a high conversion. This is problematic because both 13-HPODE and 13-HP-Endo are not stable under these conditions and decompose during prolonged reaction with singlet molecular oxygen. Therefore, the yield is low and much effort is required to isolate pure 13-HP-Endo from the complex reaction product mixture (Fig S1A, see Supporting Information) by HPLC. We designed a structurally specific synthesis of pure 13-HP-Endo (Fig. 4) that proceeded in much higher yields starting from a pure monohydroperoxide (13-HPODE) that is available through an enzymatic peroxidation of linoleic acid (23). The hydroperoxy group was protected by treatment with 2-methoxypropene and a catalytic amount of pyridinium p-toluene sulfonate (PPTs) (24). The α-methoxyisopropyl (MiP) protected hydroperoxy endoperoxide 13-HP-Endo-MiP was obtained after reaction of 13-HP-MiP with singlet molecular oxygen. Then PPTs-catalyzed deprotection in methanol delivered the final product 13-HP-Endo. Introduction of the protecting group lengthens the synthesis compared to direct reaction of 13-HPODE with singlet molecular oxygen. However, the extra steps are worthwhile because the MiP protected hydroperoxides are quite stable under the reaction conditions, and the desired product is obtained in good yield from a relatively simple product mixture (Fig S1B). The MiP protecting group is also valuable for the synthesis of a linoleate-derived hydroperoxy endoperoxide phosphocholine ester (*vide infra*).

Authentic samples of several likely fragmentation products 9-hydroxy-12-oxo-10-dodecenoic acid (HODA), 9-keto-12-oxo-10-dodecenoic acid (KODA) and 8-(2-furyl)octanoic acid (FOA) were prepared as described previously (25–27). The butenolide, 8-(5-oxo-2,5-dihydrofuran-2-yl)octanoic acid (ODFO), was prepared from the furan FOA (Fig 5). Oxidation of FOA in the presence of sodium chlorite in a slightly acidic aqueous solution at room temperature generates hydroxy butenolide HODFO (28). The cyclic forms of such hydroxy butenolide compounds are not stable, and can open to form 4-oxo-2 (Z) alkenoic acids depending on pH (28). Sodium borohydride can effectively reduce the free keto group into a hydroxyl group, and after cyclization under acidic conditions gives the butenolide compound ODFO (29).

MS/MS similarity of two expected products, KODA and ODFO, from fragmenation of 13-HP-Endo

LC-ESI/MS/MS was chosen to monitor the reaction profile. This technique allows simultaneous quantification of each specific product based on selected reaction monitoring (SRM), i.e., monitoring unique transitions between the mass-to-charge (m/z) ratio of the parent ion ($[M - H]^-$ or $[M + H]^+$) and characteristic daughter ions for each species, as well as their characteristic LC retention time that could be established using authentic samples prepared by unambiguous syntheses. The technique gives specific peaks with high signal to noise ratio, and is suitable for quantification. During the development of an MS/MS protocol for monitoring the fragmentation of 13-HP-Endo, we found that ODFO has an ESI-MS/MS spectrum similar to that of KODA. Both KODA and ODFO have isobaric parent ions and nearly identical patterns of daughter ions (Fig. 6A and B). The slight differences between the mass spectra of these two molecules are that KODA produces a dominant daughter ion at m/z 109 and a weak daughter ion at m/z 110 while ODFO gives a dominant daughter ion at m/z 110. Possible fragments that may correspond to these daughter ions are presented in Fig. 6. Furthermore, KODA and ODFO exhibited the same LC retention times when eluting with methanol and water. Although the mass spectra of both molecules show peaks in the 225 → 110 and 225 → 109 channels with reversed intensity, it is difficult to distinguish them in a mixture (Fig 6C). We subsequently found that, with an acetonitrile and water LC eluant

system, these two compounds are well separated and show the expected reversed intensity in the two channels (Fig 6D). The LC-MS/MS similarity of KODA and ODFO provides a good example that demonstrates the importance of having authentic samples, obtained through unambiguous chemical synthesis, to confirm the putative identities of molecules characterized by LC-MS/MS.

Vitamin E promotes the fragmentation the hydroperoxy endoperoxide 13-HP-Endo

It was anticipated that vitamin E (α-tocopherol), that can inhibit free radical-induced oxidation by hydrogen atom transfer that neutralizes reactive radicals, would prevent the oxidative destruction of HODA, e.g., to produce ODFO and KODA. The linoleate-derived hydroperoxy endoperoxide 13-HP-Endo was incubated at 37 °C as a dry film in open glass vials in the absence or in the presence of one equivalent of vitamin E (α-tocopherol). The amounts of potential fragment products (HODA, ODFO, KODA, FOA) were monitored by LC-ESI/MS/MS (Fig. 7). In the absence of α-tocopherol only a small amount of ODFO was slowly generated during the incubation (yield < 3%). The addition of α-tocopherol greatly promotes the fragmentation of 13-HP-Endo and increases the yields of HODA, ODFO and FOA. A large increase in the generation of HODA was found. The yield of HODA increased from below 0.2% to more than 4%, a more than 20 fold increase. The yield of ODFO also increased from below 3% to more than 8%. Furthermore, in the presence of α-tocopherol, the generation of these fragmentation products was very fast. The yields of HODA and ODFO reach their maxima in less than 2 hours. The amount of HODA decreases during further incubation due to additional oxidation and fragmentation. Compared with HODA, ODFO was relatively stable and the yield only slightly decreased during further incubation. KODA is not a major product in the fragmentation of hydroperoxy endoperoxide 13-HP-Endo under these conditions. Only small amounts of KODA were generated, possibly due to the further oxidation of HODA, during the incubation (< 0.2%) even in the presence of α-tocopherol. The yield of the furan compound FOA also increased with addition of α-tocopherol and reached its maximum after 4 hours of incubation.

HODA and ODFO are two major products from the fragmentation of 13-HP-Endo in the presence of Vitamin E. To verify their identities, two derivatizations were applied. An authentic sample of HODA and the fragmentation reaction product mixture from 13-HP-Endo were both derivatized with methoxylamine hydrochloride in pyridine. The methoxime derivative of HODA ($[M-H]^-$, m/z 256) gives a dominant daughter ion m/z 197. For the HPLC analysis, the HODA methoxime derivative was detected by ESI-MS/MS using SRM monitoring of the 225 → 197 mass transition. Before derivatization, HODA was detected in the reaction product mixture from 13-HP-Endo by ESI-MS/MS using SRM monitoring of the 227 → 84 mass transition. After derivatization, the HODA peak disappeared and the HODA methoxime derivative was detected (Fig S2). The generation of ODFO from 13-HP-Endo was further confirmed by pentaflurobenzyl (PFB) esterification. ODFO-PFB ammonia adduct ($[M+18]^+$, m/z 424) gives characteristic daughter ions with m/z 181 and m/z 163. The HPLC chromatogram of ODFO-PFB was monitored by ESI-MS/MS with SRM of the 424 → 181 mass transition. Reaction with PFB-Br caused the disappearance of ODFO. The concomitant formation of ODFOPFB from the putative ODFO generated by fragmentation of 13-HP-Endo was confirmed through comparison with an authentic sample (Fig S3).

Vitamin E stoichiometrically induces decomposition of 13-HP-Endo

To further understand the role of α-tocopherol in the decomposition of the hydroperoxy endoperoxide, we incubated 13- HP-Endo in the presence of various amounts of α-tocopherol at 37 °C for 2 hours as a dry film, and monitored the yields of HODA and ODFO simultaneously (Fig 8). The yields of HODA and ODFO are greatly increased by the addition of α-tocopherol and plateau after addition of one equivalent. The stoichiometry is

consistent with a mechanism in which α-tocopherol transfers an electron to the hydroperoxy group to generate an alkoxyl radical. Such chemistry has not been reported previously for α-tocopherol. However, it is pertinent to note that vitamin C is reported to promote fragmentation of hydroperoxides through a reductive homolysis pathway (30).

On the other hand, reductive cleavage of hydroperoxides to generate alkoxyl radicals can be induced by redox active metal ions, e.g., through a Fenton reaction. We previously showed that electron transfer from α-tocopherol reduces Fe^{3+} to its Fe^{2+} that then reductively cleaves hydroperoxides and, therefore, Fe^{n+} can catalyze the reductive homolysis of hydroperoxides by α-tocopherol (31). Catalysis by redox active metal ions is especially likely *in vivo* because, e.g., sugar-derived N-(carboxymethyl)lysine (CML) oxidative modifications in proteins bind metal ions, and these protein-bound metal ions can catalyze oxidation of ascorbate by H_2O_2 (32, 33). Electron transfer from (oxidation of) ascorbate or α-tocopherol would be accompanied by electron transfer to (reduction of) metal ions. The reduced metal ions would subsequently be reoxidized by electron transfer to H_2O_2 or to lipid hydroperoxides. It is likely that, in the presence of vitamin E, protein-bound redox active metal ions can catalyze the fragmentation of hydroperoxy endoperoxides to deliver toxic γ-hydroxyalkenals (Fig. 9).

Although metal ions were not added to the incubation of hydroperoxy endoperoxide 13-HP-Endo, it is conceivable that, in the presence of α-tocopherol, traces of redox active metal ions, e.g., Fe^{n+}, efficiently catalyze these reactions (Fig. 10). As proposed in Fig. 10, metal ion-induced reductive cleavage of the hydroperoxy endoperoxide would produce an alkoxyl radical that can further fragment to a γ-alkoxyl-α,β-unsaturated aldehyde – that gives rise to HODA, ODFO and FOA – or can be trapped by hydrogen atom transfer to form the hydroxy endoperoxide 13-H-Endo. The competition between these alternatives would depend on the rate constants k_1 and k_2 and the concentration of accessible hydrogen atom donors such as α-tocopherol (34). We expected that an excess of vitamin E (up to five equivalents) would reduce the yields of fragmentation products because it would favor production of the hydroxy endoperoxide. One possible explanation for the lack of a decrease in the yields of those products is that the rate constant k_2 is much larger than k_1. This seems likely since the β-scission with concomitant homolysis of a dialkyl hydroperoxide is expected to be very favorable owing to the simultaneous formation of two new carbonyl groups (Fig. 3). This scenario is consistent with the belief that α-tocopherol is not an efficient scavenger for hydroxyl or alkoxyl radicals *in vivo* (35).

DTPA, a metal ion-chelating agent, suppresses vitamin E-induced fragmentation of 13-HP-Endo

To test the hypothesis that traces of redox active metal ions are required for vitamin E-promoted fragmentation of 13-HP-Endo, diethylene triamine pentaacetic acid (DTPA) was introduced into our system. It was reported previously that after chelation, redox active metal ions are relatively resistant to reduction and thus lose the ability to react with α-tocopherol (36, 37). If the fragmentation were metal ion independent, the addition of DTPA would not affect the reaction. We incubated a mixture of DTPA and the hydroperoxy endoperoxide with various amounts of α-tocopherol at 37 °C for 2 hours as a dry film. The addition of DTPA totally quenched the generation of HODA and greatly suppressed the generation of ODFO (Fig. 8). This supports our hypothesis that the fragmentation is metal ion-dependant (31). We favor this explanation over the possibility that DTPA suppresses the direct reduction of hydroperoxy endoperoxides by tocopherol in some unprecedented alternative manner.

γ-Tocopherol-promoted decomposition of 13-HP-Endo causes less fragmentation than α-tocopherol

The term “vitamin E” designates a group of tocopherols and tocotrienols. Among them, α-tocopherol has been most studied, and is often said to have the highest biological activity (38). However, recent studies indicate that γ-tocopherol, the major form of vitamin E in the US diet, has some unique biological activities, such as trapping electrophilic mutagens (39), and thus may be important to human health (38, 40, 41). It is also found that γ-tocopherol does not reduce Cu(II) as rapidly as α-tocopherol, partly owing to its lack of one methyl substituent on the chromanol head group (Chart 1) (35, 42). Incubation of the hydroperoxy endoperoxide 13- HP-Endo with various amounts of γ-tocopherol at 37 °C for 1.5 hours as a dry film generated HODA and ODFO, but in lower yields than with α-tocopherol (Fig 11). Presumably, the lower reducing ability of γ-tocopherol results in less fragmentation products. This suggests the possibility that replacement of α-tocopherol with γ-tocopherol may result in less pro-oxidant effects *in vivo*.

Synthesis of hydroperoxy endoperoxide phosphocholine ester 13-HP-Endo-PC

In vivo, polyunsaturated fatty acids (PUFAs) are present mainly esterified, for example, in phospholipids. Therefore, we prepared the hydroperoxy endoperoxide phosphocholine ester 13-HP-Endo-PC through chemical synthesis (Fig. 12). The 2-methoxyisopropyl (MiP) derivative of 13-HPODE, 13-HP-MiP, could be esterified to 2-lyso-PC in the presence of dicyclohexylcarbodiimide (DCC) and 4-dimethylaminopyridine (DMAP) (43). Then reaction with singlet molecular oxygen, followed by removal of the MiP protecting group, delivered the title compound 13-HP-Endo-PC. The MiP protecting group is very important for the overall success of the synthesis because the reaction with singlet molecular oxygen proceeds very slowly, and was not complete even after 4 days of irradiation. With the protecting group, the hydroperoxy endoperoxide derivative 13-HP-Endo-PC-Mip is easily separated from the starting material, 13-HP-PC-MiP, and other oxidation products (Fig S4). 2-Methoxypropene also has been used recently as protecting group to prepare other lipid hydroperoxides (44). The potential fragmentation product HODA-PC was prepared as previously described (25) and ODFO-PC was prepared through direct esterification of ODFO.

Fragmentation of 13-HP-Endo-PC in unilamellar vesicles

To evaluate the fragmentation of hydroperoxy endoperoxide 13-HP-Endo-PC in a model membrane under physiologically relevant conditions, we incubated unilamellar vesicles comprised of 13-HP-Endo-PC (10 wt%) and 1-stearoyl-2-palmitoyl-*sn*-glycero-3-phosphocholine (SP-PC) as carrier (1:9 respectively) in pH 7.4 aqueous buffer at 37°C for various times. Only a low yield of ODFO-PC was generated (Fig. 13), even after six hours. When α-tocopherol is embedded in liposomes, the chromanol head of vitamin E is close to the interface of the aqueous phase and the bilayer membrane (Fig. 14) (45). Incubation of the above unilamellar vesicles containing α-tocopherol (one equivalent), generated both HODA-PC and ODFO-PC in greatly increased yields, reaching maxima of 7% and 9% respectively. The addition of DTPA effectively inhibited the generation of both HODA-PC and ODFO-PC, even in the presence of tocopherol. The effects of DTPA and tocopherol are similar those observed with the free acid 13-HP-Endo. In the present study it appears that redox active metal ions in the environment catalyze the reductive cleavage of the hydroperoxde group leading to fragmentation of the hydroperoxy endoperoxide13-HP-Endo-PC under biomimetic conditions.

A membrane environment protects γ-hydroxyalkenals against oxidation to butenolides

The product distribution between γ-hydroxyalkenal (HODA, HODA-PC) and their butenolide oxidation products (ODFO, ODFO-PC) exhibits interesting differences. Fragmentation of 13-HP-Endo in the homogeneous environment of a dry film gave HODA and ODFO in a 1:2–3 ratio. In contrast, the fragmentation of 13-HP-Endo-PC in a model membrane delivered HODA-PC and ODFO-PC in about a 1:1 ratio. Apparently, a membrane environment protects the γ-hydroxyalkenal against oxidation to a butenolide.

To further test this hypothesis, we incubated 13-HP-Endo-PC (10 wt%), SP-PC (90 wt%) and one equivalent α-tocopherol in a homogeneous solution in methanol and PBS buffer (1:1) at 37°C for 4 h. The yields of HODA-PC and ODFO-PC are presented in Fig. 15 and are compared to the yields obtained from the corresponding reaction in a model membrane (SUV). In homogeneous solution, the product distribution from fragmentation of 13-HP-Endo-PC is very similar to that obtained from fragmentation of 13-HP-Endo (the free acid) in a dry film, and not like that obtained from 13-HP-Endo-PC in a model membrane. This supports the hypothesis that the membrane environment protects HODA-PC against further oxidation.

Discussion

A membrane environment compartmentalizes lipid oxidation intermediates and products

As detailed in the mechanism of Fig. 3 (see above), fragmentation of the hydroperoxy endoperoxide generates an unstable cis γ-hydroxyalkenal, which can isomerize into a trans γ-hydroxyalkenal or be converted, through further oxidation, into a butenolide. Notably, the ratio of γ-hydroxyalkenal to butenolide will depend on the oxidative environment. The lipid whisker model (1, 46, 47) predicts segregation of the γ-hydroxyalkenal from lipid hydroperoxide oxidants in the membrane environment, and this favors the accumulation of HODA-PC at the expense of ODFO-PC. Thus, when cellular membranes undergo peroxidation, lipid hydroperoxides, e.g., 13-HPODE-PC (Fig. 14), remain buried in the hydrophobic core of the membrane. However, the PUFA side chain containing the hydroperoxide becomes more hydrophilic after further oxidation and truncation, and moves from the interior of the lipid bilayer to the aqueous exterior. Consequently, the membrane “grows lipid whiskers” on its surface. The model predicts that the oxygenated acyl groups of 13-HP-Endo-PC and its precursor 13-HPODE-PC prefer to remain embedded in the lipophilic core of the membrane bilayer (because they are relatively hydrophobic as indicated by the octanol/water partition coefficients log P = 4.85 and 5.59) while the more polar γ-hydroxyalkenal acyl group (log P = 1.59) of HODA-PC prefers to extend into the aqueous phase (Fig. 14). Cis-HODA-PC (see Fig. 14) partitions between isomerization to the trans isomer and oxidation to ODFO-PC. Oxidation would be disfavored in the membrane environment if lipid hydroperoxides, e.g., 13-HP-Endo-PC and 13-HPODE-PC, are required for the oxidation because the hydroperoxide of 13-HPendo-PC and the γ-hydroxyalkenal acyl group of HODA-PC are localized in different phases, i.e., membrane hydrophobic core and aqueous phase respectively. In contrast, the reaction of 13-HP-Endo-PC in an aqueous homogeneous environment (methanol/PBS, 1:1) or the reaction of 13-HP-Endo in the homogeneous environment of a dry film favors oxidation of *cis*-HODA-PC to ODFO-PC or of *cis*-HODA to ODFO because both *cis*-HODA and 13-HP-Endo or their PC esters are in the same phase.

To understand the free radical-induced oxidative transformations of PUFAs in vivo, it is essential to investigate their chemistry when they are incorporated into phospholipids in membranes because the chemistry of the free fatty acids does not recapitulate their behavior in membranes. The structure and composition of the membrane environment profoundly

influences product evolution. Previous studies of model membranes constructed from pure phospholipids, available by our unambiguous syntheses, established that the hydroperoxydiene modifications of PUFAs esterified into phospholipids – that are the major initial products of free radical- or singlet oxygen-mediated oxidation – remain buried in the hydrophobic membrane core. With further oxidation and truncation, oxidized acyl groups become hydrophilic, and adopt a conformation in which the oxidized acyl group protrudes from the membrane into the aqueous phase. Hydroperoxydienes are sources of chain-carrying alkoxy radicals that can either abstract doubly allylic hydrogen to generate pentadienyl radical precursors of additional hydroperoxides or abstract aldehydic hydrogen resulting in the oxidation of aldehydes to carboxylic acids.

Potential contributions of vitamin E and ascorbate to promoting oxidative injury

It has been more than eighty years since vitamin E was first discovered (48). Yet the role and importance of vitamin E *in vivo* is still unclear (49, 50). As an antioxidant, vitamin E can scavenge lipid peroxyl and alkoxyl radicals, and thus protect the membrane from oxidative damage (34, 51). However, vitamin E can also potentially contribute to oxidative injury: (1) by promoting lipid peroxidation, a prooxidant activity, that has been noted previously and (2), as found in the present study, by promoting fragmentation of oxidized lipids to generate toxic aldehydes that can, *inter alia*, modify proteins by covalent adduction. A pro-oxidant effect of vitamin E, i.e., owing to H atom abstraction by the tocopheryl radical, is known (52), but *in vivo* this pathway may be inhibited by coantioxidants, e.g., ascorbate. It was proposed that a deficiency of coantioxidants rather than α-tocopherol-mediated peroxidation alone may be responsible for lipoprotein lipid peroxidation in the aortic subendothelial space (53). Indeed, in several animal models of atherosclerosis, administration of bisphenol, which is a kinetically inferior classical radical scavenger, yet efficient coantioxidant that can neutralize tocopheryl radicals, dramatically lowered aortic lipoprotein lipid peroxidation (53).

Vitamins C and E, can reduce metal ions that, paradoxically, can lead to oxidation of PUFAs. For example, a prooxidant effect of α-tocopherol may arise from either metal-catalyzed or direct electron transfer to lipid hydroperoxides. The resulting reductive cleavage generates hydroxyl and/or alkoxyl radicals that can initiate free radical chain reactions between PUFAs and oxygen. In other words, α-tocopherol might promote oxidation of PUFAs by oxygen because it can cause single electron reduction of hydroperoxides and consequently generate free radical initiators of autoxidation. It was reported that α-tocopherol reduces Cu(II) to Cu(I) and concomitantly induces autoxidation in human lipoproteins (54–60). This prooxidant effect of vitamin E was presumed to be "mediated by its capability to reduce Cu^{2+} to Cu^{+} which, in turn, produces, from lipid hydroperoxides, the highly reactive alkoxyl radicals" (55). Similarly, H_2O_2 was previously shown to generate hydroxyl radicals and oxidize ascorbate ~4 times faster in the presence of proteins from cataractous lens than similar proteins from normal lens. This is presumably because the endogenous level of Cu is significantly higher in cataractous lens than in normal lens. Ascorbate oxidizing activity at 24 hours of crystallins, a structural lens protein, was significantly higher for crystallins isolated from cataractous lenses than from normal eyes. The metal ion chelator DTPA completely prevented this oxidation up to 24 hours of incubation. Presumably, the oxidation of ascorbate reduces Cu(II) to Cu(I) that then reductively cleaves H_2O_2 to generate hydroxyl radicals.

The possible contribution of hydroperoxy endoperoxide fragmentation to oxidative injury in the eye

The present study shows that vitamin E can promote the *fragmentation* of hydroperoxy endoperoxides, products that may be generated in the retina from the reaction PUFAs with

singlet molecular oxygen, to give toxic aldehydes. These can, in turn, react with proteins, leading to oxidative lipid-derived protein modifications, such as the carboxyethylpyrrole (CEP) derivatives that trigger angiogenesis into the retina, as well as an immune-mediated destruction of the retina. Therefore, the use of vitamin E as a supplement in clinical trials as a therapeutic intervention to prevent oxidative injury should not only consider its antioxidant, but also its prooxidant effects (61, 62) and its ability to promote the generation of toxic aldehydes through fragmentation of peroxidized lipids. Strong evidence is accumulating for a major role for lipid oxidation and lipid-derived protein modification in the pathogenesis of AMD. It seemed reasonable, therefore, to expect that antioxidants would have therapeutic benefits. Tocopherol's prooxidant effects and/or its ability to promote fragmentation of peroxidized lipids may help to explain why clinical trials have concluded that vitamin E in some cases provides a little but in most cases provides no benefit in ameliorating AMD (63–65). Even if vitamin E successfully neutralizes chain carrying free radicals and free radical-induced oxidation of lipids, it may concomitantly increase levels of toxic aldehydes generated by vitamin E-induced fragmentation.

The tocopherol-induced *in vitro* fragmentations of hydroperoxy endoperoxides that we described above may involve direct electron transfer leading to reductive cleavage or a process catalyzed by traces of redox active metal ions. Such catalysis is especially likely *in vivo* because carboxymethyl lysine (CML) modifications of proteins, which have been shown to bind redox active metal ions (32, 33), are found in eyes from individuals with AMD (66) and levels are elevated in cataractous lenses (67). Furthermore, it is likely that, in the presence of vitamin E, these protein-bound redox active metal ions will catalyze the reductive fragmentation of hydroperoxy endoperoxides by tocopherols to deliver toxic γ-hydroxyalkenals which, in turn, modify proteins, e.g., to produce CEPs (Fig. 16). Mean levels of CEP adducts are ~60% higher and CML adducts are ~54% higher in AMD relative to normal controls (68, 69). It is tempting to speculate that the correlation between elevated CML and elevated CEP in AMD eyes indicates a role for CMLs in promoting the generation of CEPs. Specifically, reactions of docosahexaenoate phospholipids with singlet molecular oxygen can generate hydroperoxy endoperoxides that can be converted to CEPs through the chemistry of detailed above.

The present study provides a basis for postulating that redox active metal ions contribute to lipid-derived oxidative protein modification that may be pathogenic, e.g., promoting both "wet" and "dry" forms AMD. It also suggests a mechanism that may compromise the efficacy of dietary α-tocopoherol suplementation as a therapeutic modality. Testing these hypotheses will require, *inter alia*, comparing levels of redox active metals and tocopherols in eyes from individuals with AMD and from those with no disease. In a previous study, we found that dietary α-tocopherol supplementation offered no benefit for lowering levels of oxidative protein modifications in hemodialysis patients (62). Rather, it caused a decrease in plasma γ-tocopherol levels, presumably by competitively inhibiting uptake of γ-tocopherol from the diet. Thus, supplementation with α-tocopherol resulted in a 2-fold increase in α-tocopherol levels and a concomitant halving of γ-tocopherol levels. The finding of the present study that γ-tocopherol-promoted decomposition of 13-HP-Endo causes less fragmentation than α-tocopherol suggests that dietary supplementation with γ-tocopoherol may be superior to α-tocopoherol as a therapeutic modality to prevent oxidative injury caused by the generation of toxic aldehydes.

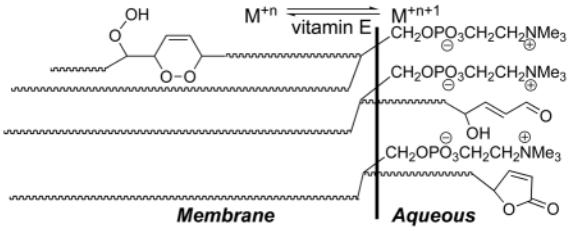

Supplementary Material

Refer to Web version on PubMed Central for supplementary material.

Acknowledgments

Funding Support. We are grateful for support of this work by National Institutes of Health Grants GM021249 and EY016813.

References

1. Greenberg ME, Li XM, Gugiu BG, Gu X, Qin J, Salomon RG, Hazen SL. The lipid whisker model of the structure of oxidized cell membranes. J Biol Chem. 2008; 283:2385–2396. [PubMed: 18045864]
2. Sun M, Finnemann SC, Febbraio M, Shan L, Annangudi SP, Podrez EA, Hoppe G, Darrow R, Organisciak DT, Salomon RG, Silverstein RL, Hazen SL. Light-induced oxidation of photoreceptor outer segment phospholipids generates ligands for CD36-mediated phagocytosis by retinal pigment epithelium: a potential mechanism for modulating outer segment phagocytosis under oxidant stress conditions. J Biol Chem. 2006; 281:4222–4230. [PubMed: 16354659]
3. Gu X, Sun M, Gugiu B, Hazen S, Crabb JW, Salomon RG. Oxidatively truncated docosahexaenoate phospholipids: total synthesis, generation, and peptide adduction chemistry. J Org Chem. 2003; 68:3749–3761. [PubMed: 12737551]
4. Kaur K, Salomon RG, O'Neil J, Hoff HF. (Carboxyalkyl)pyrroles in human plasma and oxidized low-density lipoproteins. Chem Res Toxicol. 1997; 10:1387–1396. [PubMed: 9437530]
5. Gu X, Meer SG, Miyagi M, Rayborn ME, Hollyfield JG, Crabb JW, Salomon RG. Carboxyethylpyrrole protein adducts and autoantibodies, biomarkers for age-related macular degeneration. J Biol Chem. 2003; 278:42027–42035. [PubMed: 12923198]
6. Ebrahem Q, Renganathan K, Sears J, Vasanji A, Gu X, Lu L, Salomon RG, Crabb JW, Anand- Apte B. Carboxyethylpyrrole oxidative protein modifications stimulate neovascularization: Implications for age-related macular degeneration. Proc Natl Acad Sci U S A. 2006; 103:13480–13484. [PubMed: 16938854]
7. West XZ, Malinin NL, Merkulova AA, Tischenko M, Kerr BA, Borden EC, Podrez EA, Salomon RG, Byzova TV. Oxidative stress induces angiogenesis by activating TLR2 with novel endogenous ligands. Nature. 2010; 467:972–976. [PubMed: 20927103]
8. Renganathan K, Ebrahem Q, Vasanji A, Gu X, Lu L, Sears J, Salomon RG, Anand-Apte B, Crabb JW. Carboxyethylpyrrole adducts, age-related macular degeneration and neovascularization. Adv Exp Med Biol. 2008; 613:261–267. [PubMed: 18188953]
9. Hollyfield JG, Bonilha VL, Rayborn ME, Yang X, Shadrach KG, Lu L, Ufret RL, Salomon RG, Perez VL. Oxidative damage-induced inflammation initiates age-related macular degeneration. Nat Med. 2008; 14:194–198. [PubMed: 18223656]
10. Crabb JW, Miyagi M, Gu X, Shadrach K, West KA, Sakaguchi H, Kamei M, Hasan A, Yan L, Rayborn ME, Salomon RG, Hollyfield JG. Drusen proteome analysis: an approach to the etiology of age-related macular degeneration. Proc Natl Acad Sci U S A. 2002; 99:14682–14687. [PubMed: 12391305]

11. Gugiu BG, Mesaros CA, Sun M, Gu X, Crabb JW, Salomon RG. Identification of oxidatively truncated ethanolamine phospholipids in retina and their generation from polyunsaturated phosphatidylethanolamines. Chem Res Toxicol. 2006; 19:262–271. [PubMed: 16485902]
12. Rando RR. Membrane phospholipids as an energy source in the operation of the visual cycle. Biochemistry. 1991; 30:595–602. [PubMed: 1988047]
13. Bensasson, RV.; Land, EJ.; Truscott, TG. Excited states and free radicals in biology and medicine. Oxford University Press; New York: 1993.
14. Rozanowska M, Wessels J, Boulton M, Burke JM, Rodgers MA, Truscott TG, Sarna T. Blue Light-Induced Singlet Oxygen Generation by Retinal Lipofuscin in Non-Polar Media. Free Radic Biol Med. 1998; 24:1107–1112. [PubMed: 9626564]
15. Zhang W, Sun M, Salomon RG. Preparative singlet oxygenation of linoleate provides doubly allylic dihydroperoxides: putative intermediates in the generation of biologically active aldehydes in vivo. J Org Chem. 2006; 71:5607–5615. [PubMed: 16839140]
16. Schneider C, Tallman KA, Porter NA, Brash AR. Two distinct pathways of formation of 4-hydroxynonenal. Mechanisms of nonenzymatic transformation of the 9- and 13-hydroperoxides of linoleic acid to 4-hydroxyalkenals. J Biol Chem. 2001; 276:20831–20838. [PubMed: 11259420]
17. Schneider C, Boeglin WE, Yin H, Ste DF, Hachey DL, Porter NA, Brash AR. Synthesis of dihydroperoxides of linoleic and linolenic acids and studies on their transformation to 4-hydroperoxynonenal. Lipids. 2005; 40:1155–1162. [PubMed: 16459928]
18. Neff WE, Frankel EN, Selke E, Weisleder D. Photosensitized Oxidation of Methyl Linoleate Monohydroperoxides: Hydroperoxy Cyclic Peroxides, Dihydroperoxides, Keto Esters and Volatile Thermal Decomposition Products. Lipids. 1983; 18:868–876.
19. MacDonald RC, MacDonald RI, Menco BP, Takeshita K, Subbarao NK, Hu LR. Small-volume extrusion apparatus for preparation of large, unilamellar vesicles. Biochim Biophys Acta. 1991; 1061:297–303. [PubMed: 1998698]
20. Chen X, Zhang W, Laird J, Hazen SL, Salomon RG. Polyunsaturated phospholipids promote the oxidation and fragmentation of gamma-hydroxyalkenals: formation and reactions of oxidatively truncated ether phospholipids. J Lipid Res. 2008; 49:832–846. [PubMed: 18165704]
21. Balamraju YN, Sun M, Salomon RG. Gamma-hydroxyalkenals are oxidatively cleaved through Michael addition of acylperoxy radicals and fragmentation of intermediate beta- hydroxyperesters. J Am Chem Soc. 2004; 126:11522–11528. [PubMed: 15366898]
22. Gao S, Zhang R, Greenberg ME, Sun M, Chen X, Levison BS, Salomon RG, Hazen SL. Phospholipid hydroxyalkenals, a subset of recently discovered endogenous CD36 ligands, spontaneously generate novel furan-containing phospholipids lacking CD36 binding activity in vivo. J Biol Chem. 2006; 281:31298–31308. [PubMed: 16908526]
23. Funk MO, Isacc R, Porter NA. Preparation and purification of lipid hydroperoxides from arachidonic and gamma-linolenic acids. Lipids. 1976; 11:113–117. [PubMed: 814377]
24. Dussault PH, Woller KR. Singlet Oxygenation/Radical Rearrangement as an Approach to 1,4-Dioxygenated Peroxides: Asymmetric Total Syntheses of Plakorin and enantio-Chondrillin. J Am Chem Soc. 1997; 119:3824–3825.
25. Deng Y, Salomon RG. Total Synthesis of γ-Hydroxy-α,β-Unsaturated Aldehydic Esters of Cholesterol and 2-Lysophosphatidylcholine. J Org Chem. 1998; 63:7789–7794.
26. Jian W, Lee SH, Arora JS, Silva Elipe MV, Blair IA. Unexpected formation of etheno- 2′-deoxyguanosine adducts from 5(S)-hydroperoxyeicosatetraenoic acid: evidence for a bis-hydroperoxide intermediate. Chem Res Toxicol. 2005; 18:599–610. [PubMed: 15777099]
27. Gallasch BA, Spiteller G. Synthesis of 9,12-dioxo-10(Z)-dodecenoic acid, a new fatty acid metabolite derived from 9-hydroperoxy-10,12-octadecadienoic acid in lentil seed (Lens culinaris Medik). Lipids. 2000; 35:953–960. [PubMed: 11026615]
28. Annangudi SP, Sun M, Salomon RG. An Efficient Synthesis of 4-Oxoalkenoic Acids from 2-Alkylfurans. Synlett. 2005; 9:1468–1470.
29. Teijeira M, Suarez PL, Gomez G, Teran C, Fall Y. The furan approach to oxacycles. Part 5: Synthesis of a chiral butenolide, building block towards biologically interesting natural products. Tetrahedron Letters. 2005; 46:5889–5892.

30. Lee SH, Oe T, Blair IA. Vitamin C-induced decomposition of lipid hydroperoxides to endogenous genotoxins. Science. 2001; 292:2083–2086. [PubMed: 11408659]
31. Gu X, Zhang W, Salomon RG. Fe2+ catalyzes vitamin E-induced fragmentation of hydroperoxy and hydroxy endoperoxides that generates gamma-hydroxy alkenals. J Am Chem Soc. 2007; 129:6088–6089. [PubMed: 17441719]
32. Glomb MA, Monnier VM. Mechanism of protein modification by glyoxal and glycolaldehyde, reactive intermediates of the Maillard reaction. J Biol Chem. 1995; 270:10017–10026. [PubMed: 7730303]
33. Saxena AK, Saxena P, Wu X, Obrenovich M, Weiss MF, Monnier VM. Protein aging by carboxymethylation of lysines generates sites for divalent metal and redox active copper binding: relevance to diseases of glycoxidative stress. Biochem Biophys Res Commun. 1999; 260:332–338. [PubMed: 10403771]
34. Traber MG, Atkinson J. Vitamin E, antioxidant and nothing more. Free Radic Biol Med. 2007; 43:4–15. [PubMed: 17561088]
35. Niki E, Noguchi N. Dynamics of antioxidant action of vitamin E. Acc Chem Res. 2004; 37:45–51. [PubMed: 14730993]
36. Burkitt MJ, Milne L. Hydroxyl radical formation from Cu(II)-trolox mixtures: insights into the pro-oxidant properties of alpha-tocopherol. FEBS Lett. 1996; 379:51–54. [PubMed: 8566228]
37. Hanna PM, Mason RP. Direct evidence for inhibition of free radical formation from Cu(I) and hydrogen peroxide by glutathione and other potential ligands using the EPR spin-trapping technique. Arch Biochem Biophys. 1992; 295:205–213. [PubMed: 1315504]
38. Brigelius-Flohe R, Traber MG. Vitamin E: function and metabolism. Faseb J. 1999; 13:1145–1155. [PubMed: 10385606]
39. Christen S, Woodall AA, Shigenaga MK, Southwell-Keely PT, Duncan MW, Ames BN. gamma-tocopherol traps mutagenic electrophiles such as NO(X) and complements alpha- tocopherol: physiological implications. Proc Natl Acad Sci U S A. 1997; 94:3217–3222. [PubMed: 9096373]
40. Jiang Q, Christen S, Shigenaga MK, Ames BN. gamma-tocopherol, the major form of vitamin E in the US diet, deserves more attention. Am J Clin Nutr. 2001; 74:714–722. [PubMed: 11722951]
41. Hensley K, Benaksas EJ, Bolli R, Comp P, Grammas P, Hamdheydari L, Mou S, Pye QN, Stoddard MF, Wallis G, Williamson KS, West M, Wechter WJ, Floyd RA. New perspectives on vitamin E: gamma-tocopherol and carboxyelthylhydroxychroman metabolites in biology and medicine. Free Radic Biol Med. 2004; 36:1–15. [PubMed: 14732286]
42. Yoshida Y, Niki E, Noguchi N. Comparative study on the action of tocopherols and tocotrienols as antioxidant: chemical and physical effects. Chem Phys Lipids. 2003; 123:63–75. [PubMed: 12637165]
43. Baba M, Yoneda K, Tahara S, Iwasa J, Keneko T, Matsuo M. A regioselective, stereoselective synthesis of a diacylglycerophosphocholine hydroperoxide by use of lipoxygenase and lipase. J Chem Soc, Chem Commun. 1990:1281–1282.
44. Ibusuki D, Nakagawa K, Asai A, Oikawa S, Masuda Y, Suzuki T, Miyazawa T. Preparation of pure lipid hydroperoxides. J Lipid Res. 2008; 49:2668–2677. [PubMed: 18641373]
45. Atkinson J, Epand RF, Epand RM. Tocopherols and tocotrienols in membranes: a critical review. Free Radic Biol Med. 2008; 44:739–764. [PubMed: 18160049]
46. Li XM, Salomon RG, Qin J, Hazen SL. Conformation of an endogenous ligand in a membrane bilayer for the macrophage scavenger receptor CD36. Biochemistry. 2007; 46:5009–5017. [PubMed: 17407326]
47. Govindarajan B, Junk A, Algeciras M, Salomon RG, Bhattacharya SK. Increased isolevuglandin-modified proteins in glaucomatous astrocytes. Mol Vis. 2009; 15:1079–1091. [PubMed: 19503745]
48. Evans HM, Bishop KS. On the Existence of a Hitherto Unrecognized Dietary Factor Essential for Reproduction. Science. 1922; 56:650–651. [PubMed: 17838496]
49. Brigelius-Flohe R. Vitamin E: the shrew waiting to be tamed. Free Radic Biol Med. 2009; 46:543–554. [PubMed: 19133328]
50. Azzi A. Molecular mechanism of alpha-tocopherol action. Free Radic Biol Med. 2007; 43:16–21. [PubMed: 17561089]

51. Herrera E, Barbas C. Vitamin E: action, metabolism and perspectives. J Physiol Biochem. 2001; 57:43–56.
52. Bowry VW, Ingold KU. The Unexpected Role of Vitamin E (a-Tocopherol) in the Peroxidation of Human Low-Density Lipoprotein. Acc Chem Res. 1999; 32:27–34.
53. Upston JM, Terentis AC, Stocker R. Tocopherol-mediated peroxidation of lipoproteins: implications for vitamin E as a potential antiatherogenic supplement. Faseb J. 1999; 13:977–994. [PubMed: 10336881]
54. Yamamoto K, Niki E. Interaction of alpha-tocopherol with iron: antioxidant and prooxidant effects of alpha-tocopherol in the oxidation of lipids in aqueous dispersions in the presence of iron. Biochim Biophys Acta. 1988; 958:19–23. [PubMed: 3334865]
55. Maiorino M, Zamburlini A, Roveri A, Ursini F. Prooxidant role of vitamin E in copper induced lipid peroxidation. FEBS Lett. 1993; 330:174–176. [PubMed: 8365487]
56. Yoshida Y, Tsuchiya J, Niki E. Interaction of alpha-tocopherol with copper and its effect on lipid peroxidation. Biochim Biophys Acta. 1994; 1200:85–92. [PubMed: 8031846]
57. Kontush A, Meyer S, Finckh B, Kohlschutter A, Beisiegel U. Alpha-tocopherol as a reductant for Cu(II) in human lipoproteins. Triggering role in the initiation of lipoprotein oxidation. J Biol Chem. 1996; 271:11106–11112. [PubMed: 8626654]
58. Bittner O, Gal S, Pinchuk I, Danino D, Shinar H, Lichtenberg D. Copper-induced peroxidation of liposomal palmitoyllinoleoylphosphatidylcholine (PLPC), effect of antioxidants and its dependence on the oxidative stress. Chem Phys Lipids. 2002; 114:81–98. [PubMed: 11841827]
59. Esterbauer H, Gebicki J, Puhl H, Jurgens G. The role of lipid peroxidation and antioxidants in oxidative modification of LDL. Free Radic Biol Med. 1992; 13:341–390. [PubMed: 1398217]
60. Burkitt MJ. A critical overview of the chemistry of copper-dependent low density lipoprotein oxidation: roles of lipid hydroperoxides, alpha-tocopherol, thiols, and ceruloplasmin. Arch Biochem Biophys. 2001; 394:117–135. [PubMed: 11566034]
61. Sesso HD, Buring JE, Christen WG, Kurth T, Belanger C, MacFadyen J, Bubes V, Manson JE, Glynn RJ, Gaziano JM. Vitamins E and C in the prevention of cardiovascular disease in men: the Physicians' Health Study II randomized controlled trial. Jama. 2008; 300:2123–2133. [PubMed: 18997197]
62. Lu L, Erhard P, Salomon RG, Weiss MF. Serum vitamin E and oxidative protein modification in hemodialysis: a randomized clinical trial. Am J Kidney Dis. 2007; 50:305–313. [PubMed: 17660032]
63. Jampol LM, Ferris FL 3rd. Antioxidants and zinc to prevent progression of age-related macular degeneration. Jama. 2001; 286:2466–2468.
64. Kuzniarz M, Mitchell P, Flood VM, Wang JJ. Use of vitamin and zinc supplements and age-related maculopathy: the Blue Mountains Eye Study. Ophthalmic Epidemiol. 2002; 9:283–295. [PubMed: 12187426]
65. Taylor HR, Tikellis G, Robman LD, McCarty CA, McNeil JJ. Vitamin E supplementation and macular degeneration: randomised controlled trial. Bmj. 2002; 325:11. [PubMed: 12098721]
66. Ishibashi T, Murata T, Hangai M, Nagai R, Horiuchi S, Lopez PF, Hinton DR, Ryan SJ. Advanced glycation end products in age-related macular degeneration. Arch Ophthalmol. 1998; 116:1629–1632. [PubMed: 9869793]
67. Saxena P, Saxena AK, Cui XL, Obrenovich M, Gudipaty K, Monnier VM. Transition metal-catalyzed oxidation of ascorbate in human cataract extracts: possible role of advanced glycation end products. Invest Ophthalmol Vis Sci. 2000; 41:1473–1481. [PubMed: 10798665]
68. Gu J, Pauer GJ, Yue X, Narendra U, Sturgill GM, Bena J, Gu X, Peachey NS, Salomon RG, Hagstrom SA, Crabb JW. Assessing susceptibility to age-related macular degeneration with proteomic and genomic biomarkers. Mol Cell Proteomics. 2009; 8:1338–1349. [PubMed: 19202148]
69. Ni J, Yuan X, Gu J, Yue X, Gu X, Nagaraj RH, Crabb JW. Study Group, C. Plasma protein pentosidine and carboxymethyllysine, biomarkers for age-related macular degeneration. Mol Cell Proteomics. 2009; 8:1921–1933. [PubMed: 19435712]

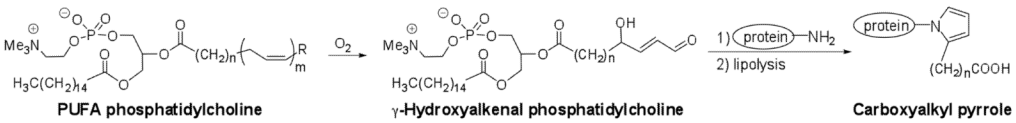

Figure 1.
Oxidative cleavage of polyunsaturated fatty acyl (PUFA) phosphatidylcholines generates γ-hydroxyalkenal phosphatidylcholines that react with proteins to deliver carboxyalkyl pyrroles.

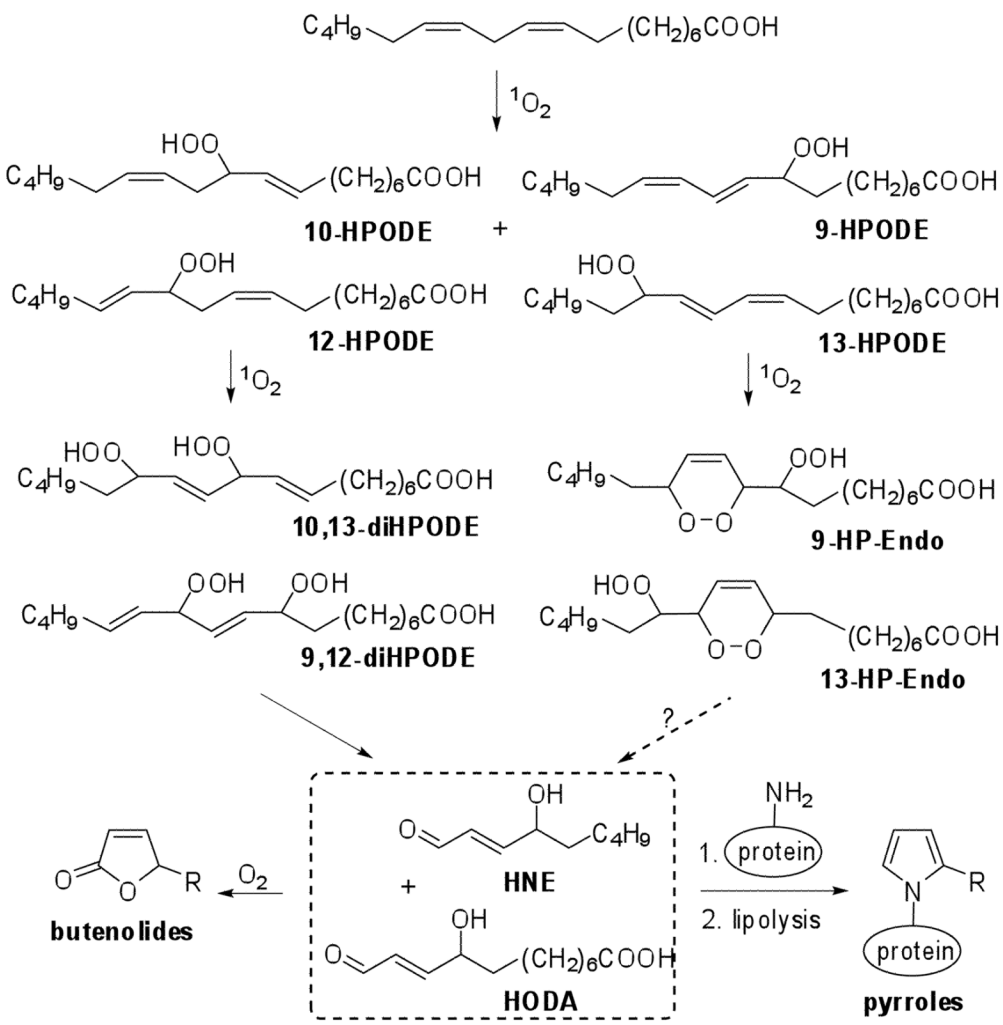

Figure 2.

Singlet molecular oxygen reaction pathways to γ-hydroxyalkenals. Further oxidation produces butenolides in competition with adduction to proteins to generate carboxyalkyl pyrroles.

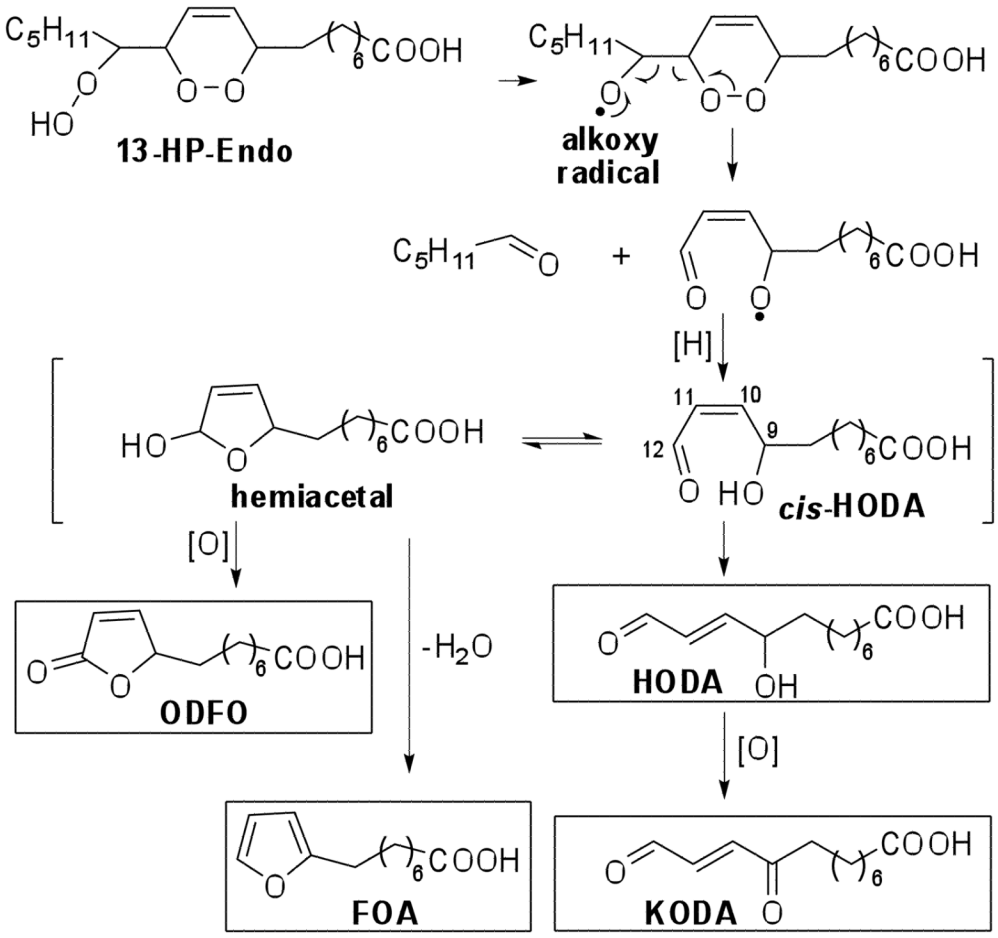

Figure 3.
Postulated fragmentation products from 13-HP-Endo.

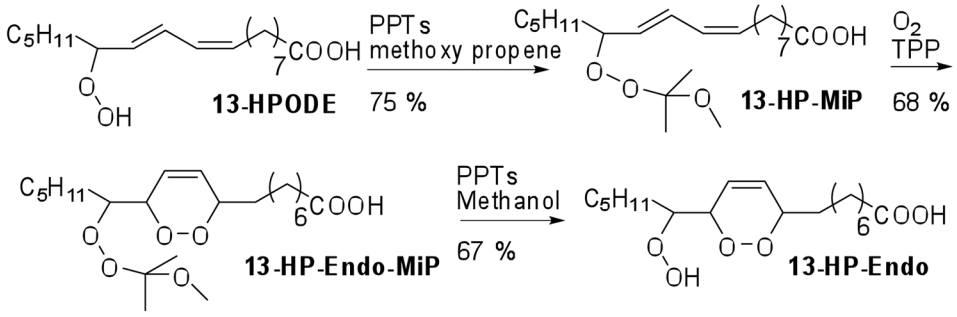

Figure 4.
Structurally specific synthesis of a 13-hydroperoxyendoperoxide.

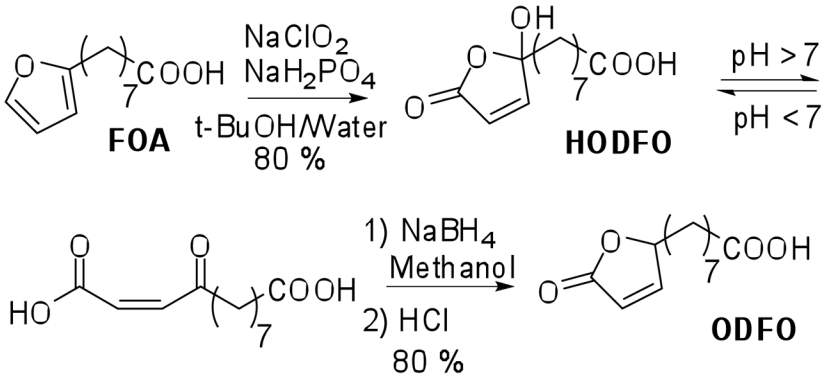

Figure 5.
Synthesis of the butenolide ODFO.

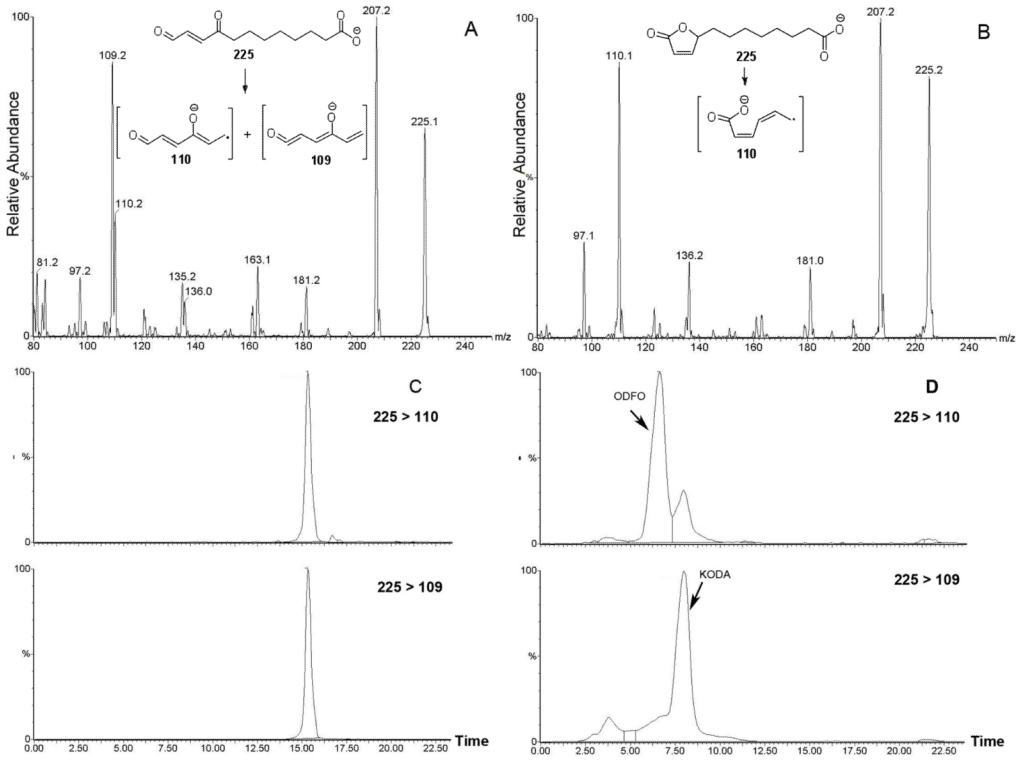

Figure 6.

Negative ESI-MS/MS spectrum of KODA (A) and ODFO (B), and HPLC chromatogram of KODA and ODFO (1:1 mixture) eluting with methanol/water (C) and acetonitrile/water (D). The chromatogram was monitored by LC-MS in the negative ion mode with SRM of appropriate mass transitions as noted.

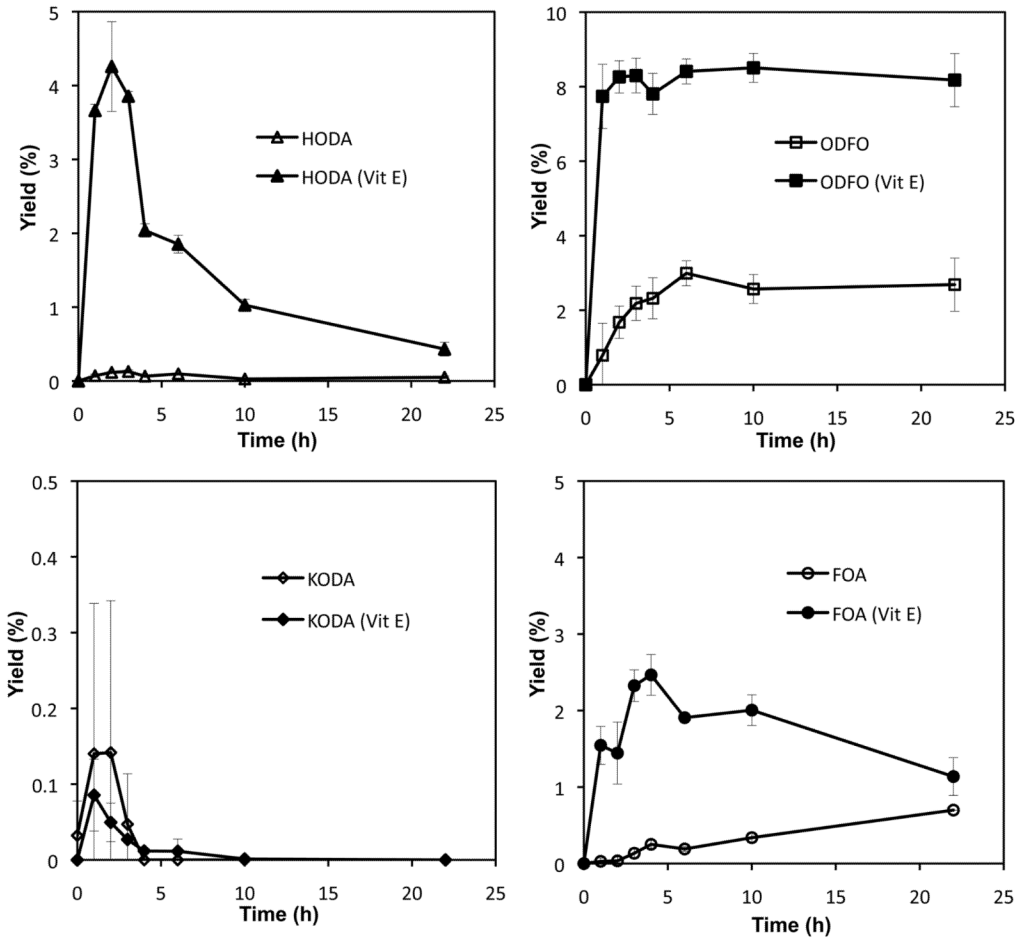

Figure 7.

Time courses for the generation of HODA, ODFO, KODA and FOA during the thermal decomposition of 13-HP-Endo in the absence (open symbols) or presence (solid symbols) of α-tocopherol (Vit E). Error bars are deviation from average of duplicate runs within less than 24 h.

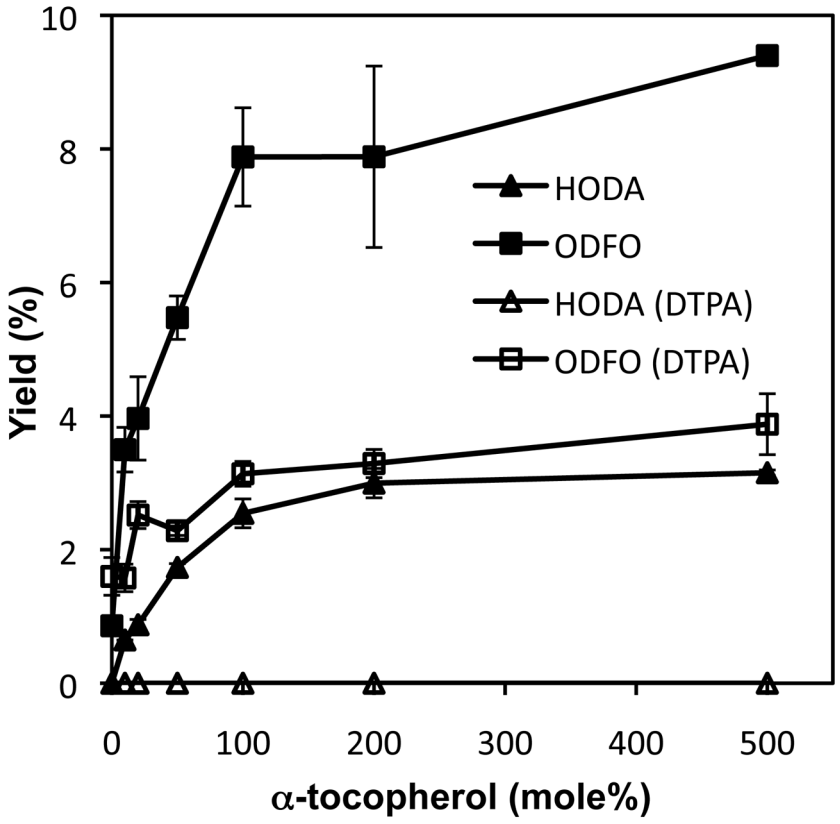

Figure 8.
Formation of HODA and ODFO from 13-HP-Endo with various amounts of α-tocopherol in the absence and presence of the chelating agent diethylene triamine pentaacetic acid (DTPA). Error bars are deviation from average of duplicate runs within less than 24 h.

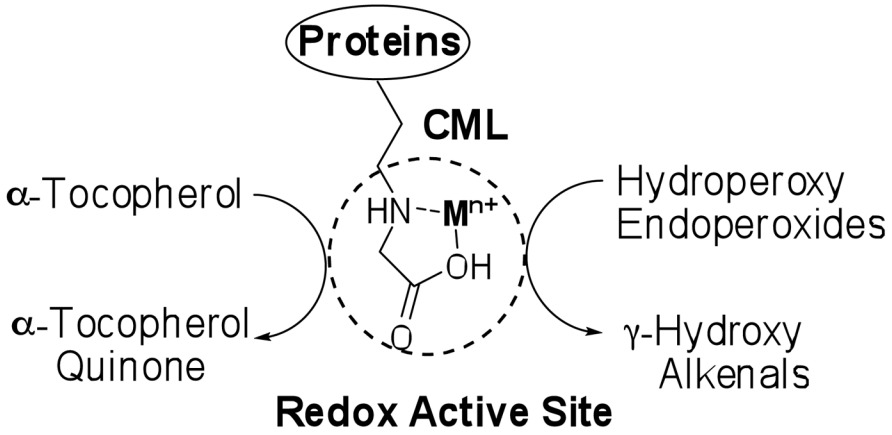

Figure 9.
CML-bound redox-active metal ions may catalyze reductive fragmentation of hydroperoxy endoperoxides to γ-hydroxyalkenals.

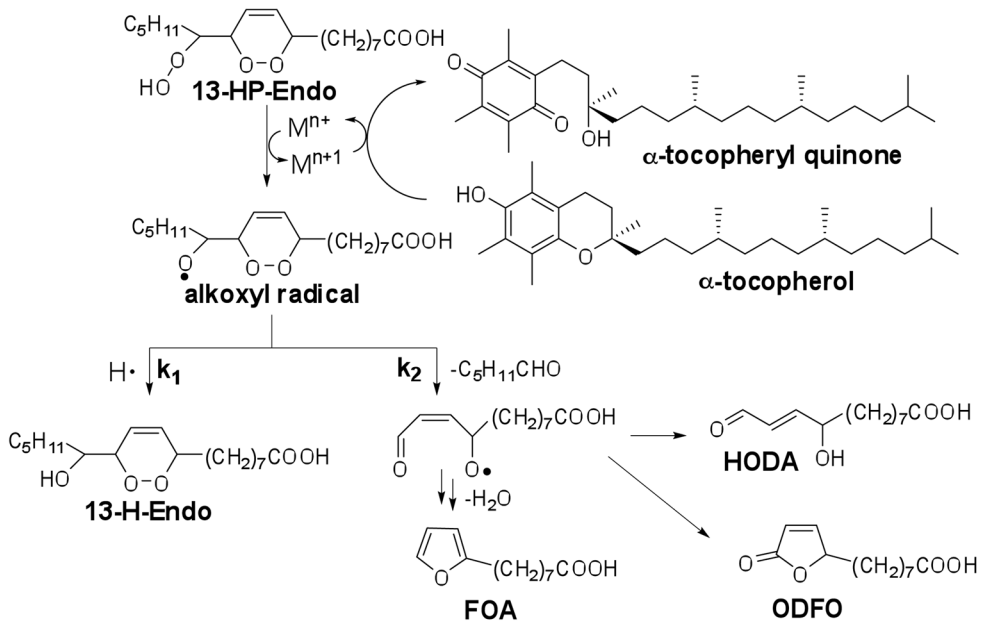

Figure 10.
A possible redox metal ion catalyzed reductive homolysis of 13-HP-Endo by α-tocopherol.

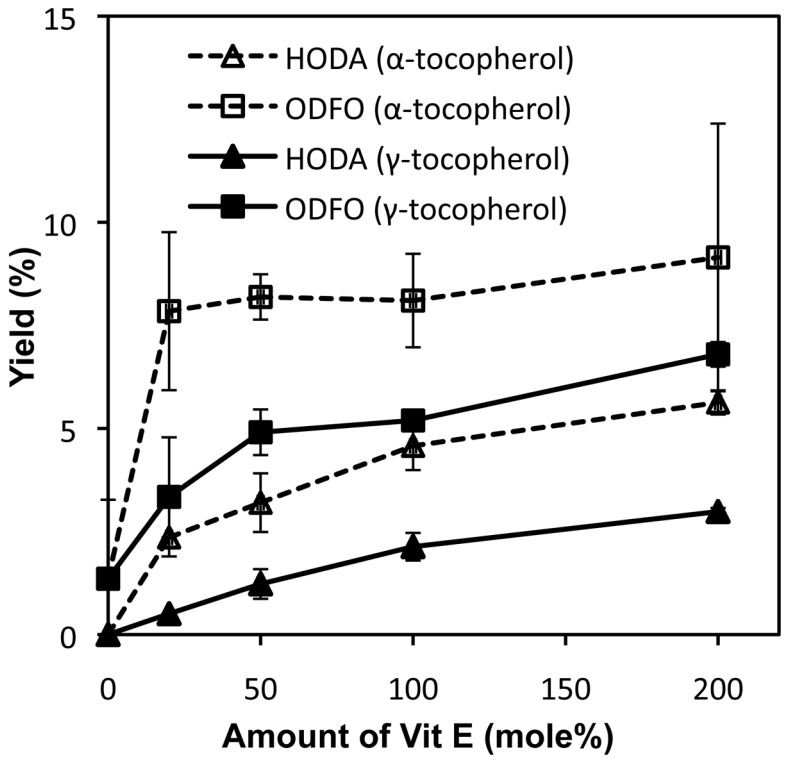

Figure 11.
Formation of HODA and ODFO from 13-HP-Endo in the presence of various amounts of α-tocopherol or γ-tocopherol.

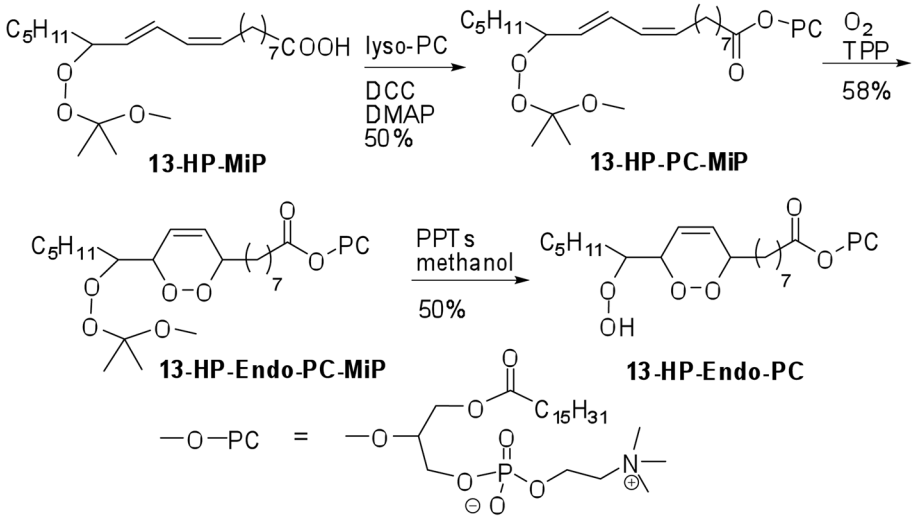

Figure 12.
Synthesis of a hydroperoxy endoperoxide phosphocholine ester 13-HP-Endo-PC.

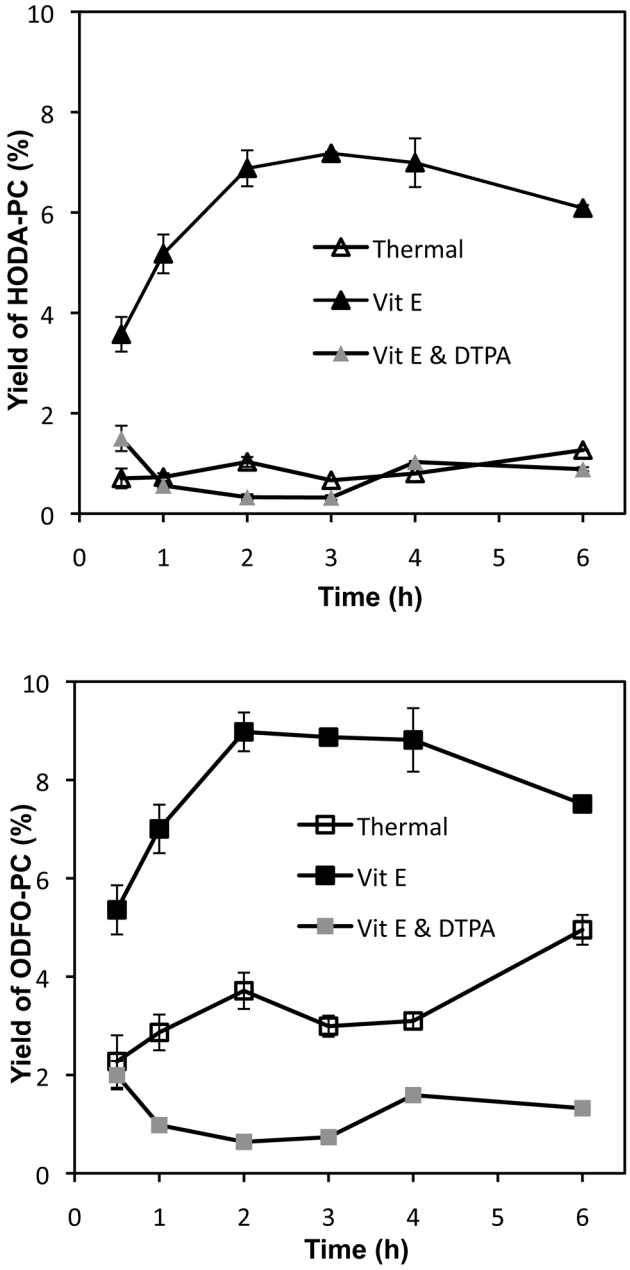

Figure 13.
Formation of HODA-PC and ODFO-PC from 13-HP-Endo-PC in small unilamellar vesicles, in PBS buffer (50 mM), with one equivalent of α-tocopherol (Vit E) in PBS buffer (50 mM), or with one equivalent of α-tocopherol in PBS buffer (50 mM) with DTPA (100 μM).

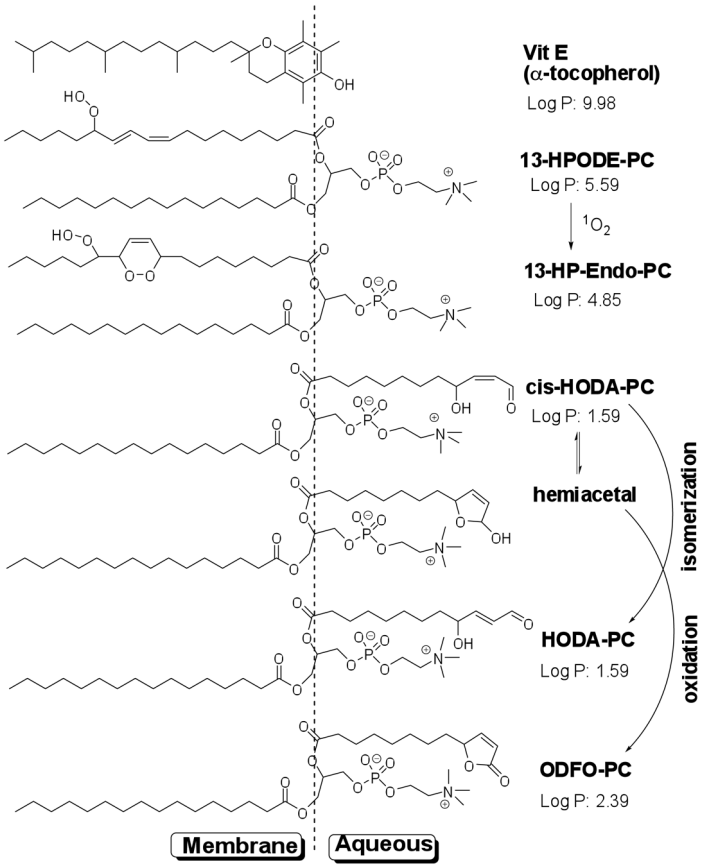

Figure 14.

Fragmentation of 13-HP-Endo-PC in unilamellar vesicles. Octanol/water partition coefficients (Log P) for α-tocopherol and the methyl esters of the oxidized PUFAs, calculated by ChemDraw®, are shown as a measure of relative hydrophobicity.

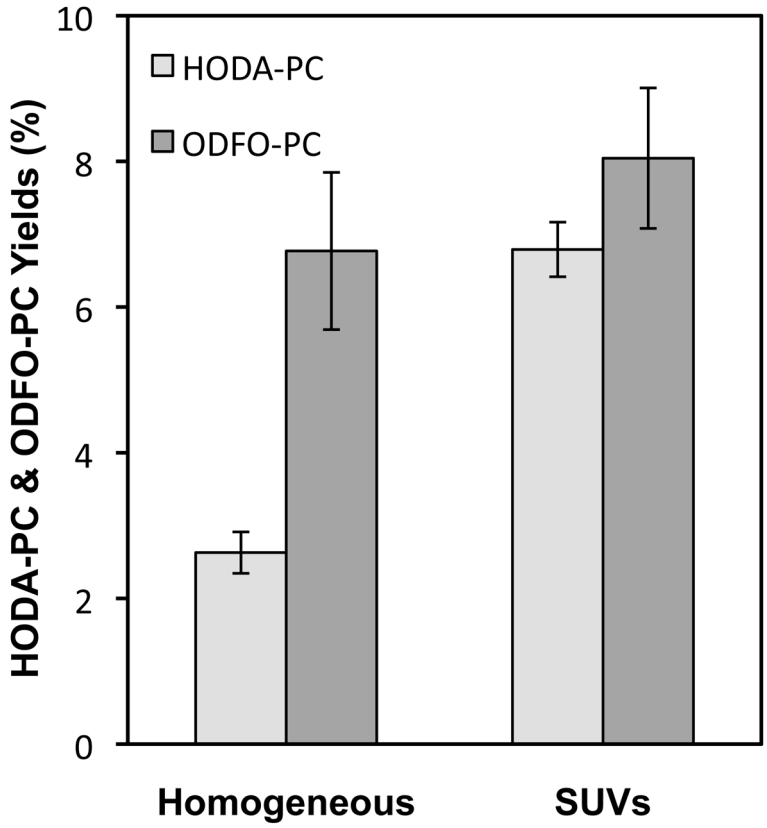

Figure 15.
Formation of HODA-PC and ODFO-PC from 13-HP-Endo-PC in methanol and buffer homogeneous solution and in small unilamellar vesicles.

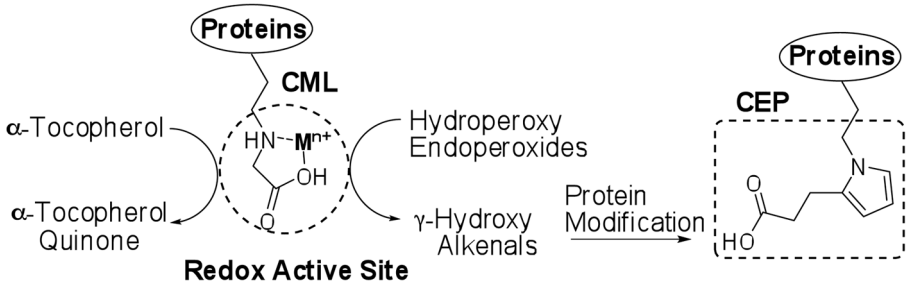

Figure 16.
Possible mechanism that links elevated carboxymethyllysine (CML) accumulation with the generation of carboxyethylpyrroles (CEPs) in the retina of AMD eyes.

Chart 1

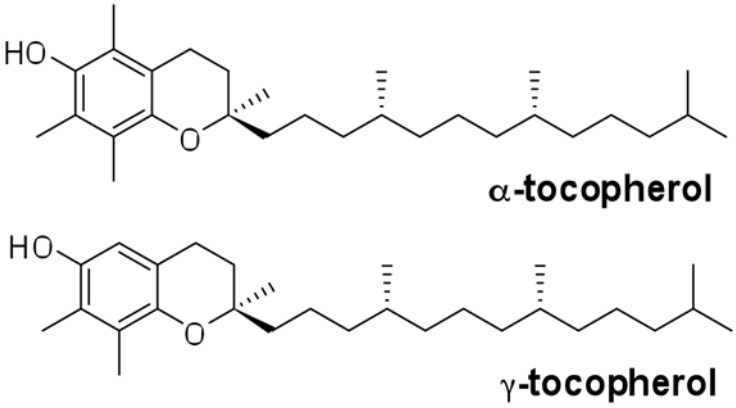

Chart 1.